Accurate Critical Buckling Load/Temperature of Thick Annular Sector Plates

A. Hasani Baferani[1] and A. R. Saidi[2]

Abstract: In this paper, stability analysis of thick annular sector plates under mechanical and thermal loads based on third-order shear deformation theory (TSDT) is investigated. The equilibrium and stability equations based on TSDT are obtained and solved analytically by doing some mathematical manipulation. Then, for nine possible boundary conditions, the buckling load and temperature are calculated and compared with those obtained using different plate theories. As the results show, for boundary conditions that include simply supported and clamped edges, the minimum value for buckling load and temperature is predicted by first-order shear deformation theory (FSDT) and maximum value is predicted by classical plate theory (CPT). Also, for boundary conditions containing free edges, the value obtained by TSDT is larger than that obtained using CPT and FSDT for some values of thickness/length ratio. It is worthy to mention that the results obtained from CPT for boundary conditions containing free edges in a wide range of thickness/length ratio are acceptable. **DOI: 10.1061/(ASCE)EM.1943-7889.0000372.**

CE Database subject headings: Buckling; Plates; Analytical techniques; Temperature effects; Thermal factors.

Author keywords: Buckling plates; Analytical techniques; Stability criteria.

Introduction

The higher-order shear deformation theories for thick plates have been investigated by Levinson (1980) and Reddy and et al. (1984a, 1985). These theories involve higher-order terms in the Taylor expansion of displacements in the thickness coordinate. The first-order shear deformation plate theory was first presented by Reissner (1945) and Mindlin (1951). It has been assumed that the in-plane displacements through the thickness of the plate are linear functions. There are essentially two limitations in the first-order shear deformation theory (FSDT):namely, that there is the inconsistency in the shear stress distribution through the thickness, and that the shear-free boundary conditions on the top and bottom surfaces of the beam or plate are not satisfied. To rectify these limitations, the higher-order shear deformation theories have been recommended (Reddy and Phan 1985).

Reddy (1984b) developed a simple, higher-order shear deformation theory for laminated composite plates. He presented the exact closed-form solutions for symmetric, cross-ply laminates and showed that the deflections and stresses predicted by his theory correlated better with the exact three-dimensional elasticity theory than those predicted by the first-order theory. In the third-order shear deformation theory (TSDT), the in-plane displacement components are assumed to take cubic expansions in the thickness direction.

[1]Ph.D. Student, Mechanical Engineering Dept., Amirkabir Univ. of Technology, Hafez Ave., 424, Tehran, Iran.

[2]Associate Professor, Dept. of Mechanical Engineering, S. Bahonar Univ. of Kerman, Kerman, Iran (corresponding author). E-mail: saidi@mail.uk.ac.ir

Note. This manuscript was submitted on August 9, 2010; approved on December 8, 2011; published online on December 12, 2011. Discussion period open until November 1, 2012; separate discussions must be submitted for individual papers. This paper is part of the ***Journal of Engineering Mechanics***, Vol. 138, No. 6, June 1, 2012. ©ASCE, ISSN 0733-9399/2012/6-614–630/$25.00.

The subject of buckling and thermal buckling of plates has been extensively studied in the literature. Using the numerical methods, some authors studied the buckling and thermal buckling of annular sector plates (Rubin 1978; Srinivasan and Thiruvenkatachari 1984; Navaneethakrishnan 1988; Liu and Chen 1989; Wang et al. 1994; Zhou et al. 1995; Ni et al. 2005; Sharma et al. 2005a, b). Reddy and Phan (1985) presented stability and vibration of simply supported rectangular plates according to a higher-order shear deformation theory. They concluded that the results presented by TSDT predict the frequencies and buckling loads more accurately compared with the FSDT and classical plate theory (CPT). Nosier and Reddy (1992a, b) investigated the free vibration and buckling problems of rectangular plates with transversely isotropic layers based on CPT, FSDT, and TSDT, respectively. Wang and Lee (1998) studied the buckling analysis of axisymmetric circular plates, and they presented an exact relationship between the buckling load of circular plates based on CPT and that of TSDT.

Wang and Xiang (1999) proposed a relationship for the buckling loads of sectorial plates obtained from CPT and FSDT. Some relationships for the buckling load of circular and sector plate based on the CPT, FSDT, and TSDT have been presented in the text book by Wang et al. (2000). Javaheri and Eslami (2002) presented the thermal buckling analysis of functionally graded simply supported rectangular plates. They compared the results of classical and third-order shear deformation plate theories and concluded that the results obtained using TSDT accurately predict the buckling temperature of such plates. Samsam Shariat and Eslami (2007) presented buckling analysis of simply supported, thick, functionally graded rectangular plates under mechanical and thermal loads by using TSDT. They compared the results of CPT, FSDT, and TSDT.

By using unconstrained third-order shear deformation plate theory, Saidi et al. (2009) studied the axisymmetric bending and buckling analysis of thick, functionally graded circular plates. They concluded that the effect of vanishing transverse shear stress on top and bottom surfaces of the plate is not substantial, and thus TSDT results are satisfactorily reliable. Bodaghi and Saidi

(2010) investigated the buckling analysis of functionally graded, thick, rectangular plates based on third-order shear deformation plate theory. Naderi and Saidi (2011a) presented the buckling analysis of moderately thick, functionally graded sector and annular sector plates based on FSDT. Also, Naderi and Saidi (2011b) investigated the stability analysis of moderately thick, functionally graded sector plates resting on elastic foundation. Saidi and Hasani Baferani (2010) investigated the thermal buckling analysis of functionally graded, moderately thick, annular sector plates based on the first-order shear deformation plate theory.

In the present work, stability analysis of thick annular sector plates under mechanical and thermal loads is investigated. The equilibrium and stability equations are obtained based on the third-order shear deformation plate theory. By using an analytical method, the coupled stability equations are converted to decoupled equations. To solve the decoupled equations, it is assumed that the annular sector plate is simply supported in radial edges, and it has arbitrary boundary conditions in circular edges. By satisfying boundary conditions at the circular edges, the critical buckling load and/or temperature are obtained analytically. Comparisons for critical buckling load/temperature of the annular sector plates obtained from different plate theories (CPT, FSDT, and TSDT) are presented. The effects of boundary conditions, thickness-radius ratio, sector angle, and annularity on the buckling load/temperature of annular sector plate are discussed in detail. Finally, the range of validity of some plate theories for buckling analysis of thick, annular sector plates under different boundary conditions is investigated.

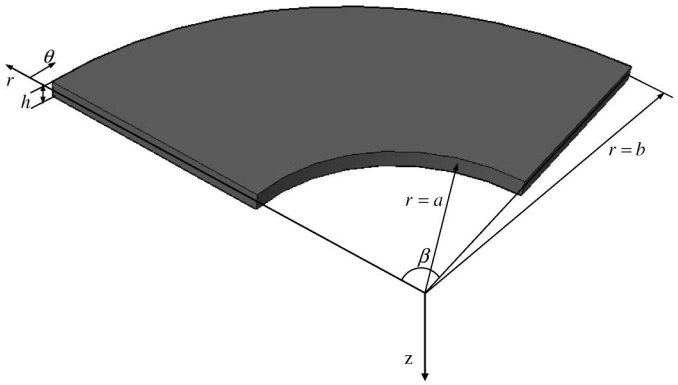

Fig. 1. Geometry and the coordinate system of a thick, annular sector plate

Equilibrium Equations

Consider a thick, annular sector plate with inner radius a, outer radius b, thickness h, and sector angle β. The geometry and coordinates are shown in Fig. 1. The displacement components, based on the third-order shear deformation plate theory, are assumed to be

$$u_r(r,\theta,z) = u(r,\theta) + z\phi_r(r,\theta) - \eta z^3\left(\phi_r(r,\theta) + \frac{\partial w(r,\theta)}{\partial r}\right) \qquad u_\theta(r,\theta,z) = v(r,\theta) + z\phi_\theta(r,\theta) - \eta z^3\left(\phi_\theta(r,\theta) + \frac{1}{r}\frac{\partial w(r,\theta)}{\partial \theta}\right)$$
$$u_z(r,\theta,z) = w(r,\theta) \tag{1}$$

where u, v, and w are the displacement components in the r, θ, and z directions, respectively; ϕ_r and ϕ_θ are the rotation functions; and $\eta = \frac{4}{3h^2}$. Based on displacement field (1), the strain-displacement relations can be expressed as

$$\varepsilon_{rr} = \frac{\partial u}{\partial r} + \frac{1}{2}\left(\frac{\partial w}{\partial r}\right)^2 + z\left(\frac{\partial \phi_r}{\partial r}\right) - \eta z^3\left(\frac{\partial \phi_r}{\partial r} + \frac{\partial^2 w}{\partial r^2}\right)$$
$$\varepsilon_{\theta\theta} = \frac{1}{r}\frac{\partial v}{\partial \theta} + \frac{u}{r} + \frac{1}{2r^2}\left(\frac{\partial w}{\partial \theta}\right)^2 + z\left(\frac{1}{r}\frac{\partial \phi_\theta}{\partial \theta} + \frac{\phi_r}{r}\right) - \eta z^3\left(\frac{1}{r}\frac{\partial \phi_\theta}{\partial \theta} + \frac{\phi_r}{r} + \frac{1}{r^2}\frac{\partial^2 w}{\partial \theta^2} + \frac{1}{r}\frac{\partial w}{\partial r}\right)$$
$$2\varepsilon_{r\theta} = \frac{1}{r}\frac{\partial u}{\partial \theta} + \frac{\partial v}{\partial r} - \frac{v}{r} + \frac{1}{r}\frac{\partial w}{\partial r}\frac{\partial w}{\partial \theta} + z\left(\frac{1}{r}\frac{\partial \phi_r}{\partial \theta} + \frac{\partial \phi_\theta}{\partial r} - \frac{\phi\theta}{r}\right) - \eta z^3\left(\frac{1}{r}\frac{\partial \phi_r}{\partial \theta} + \frac{\partial \phi_\theta}{\partial r} - \frac{\phi_\theta}{r} + \frac{2}{r}\frac{\partial^2 w}{\partial r \partial \theta} - \frac{2}{r}\frac{\partial w}{\partial \theta}\right)$$
$$2\varepsilon_{rz} = \phi_r + \frac{\partial w}{\partial r} - 3\eta z^2\left(\phi_\theta + \frac{\partial w}{\partial r}\right) \qquad 2\varepsilon_{\theta z} = \phi_\theta + \frac{1}{r}\frac{\partial w}{\partial \theta} - 3\eta z^2\left(\phi_\theta + \frac{1}{r}\frac{\partial w}{\partial \theta}\right) \tag{2}$$

where ε_{rr} and $\varepsilon_{\theta\theta}$ are the normal strains, and $\varepsilon_{r\theta}$ and $\varepsilon_{\theta z}$ are the shear strains. Using the principle of minimum total potential energy, the equilibrium equations of annular sector plate are obtained as

$$\delta u: \ \frac{\partial N_{rr}}{\partial r} + \frac{1}{r}\frac{\partial N_{r\theta}}{\partial \theta} + \frac{N_{rr} - N_{\theta\theta}}{r} = 0 \qquad \delta v: \ \frac{\partial N_{r\theta}}{\partial r} + \frac{1}{r}\frac{\partial N_{\theta\theta}}{\partial \theta} + \frac{2N_{r\theta}}{r} = 0$$
$$\delta \psi_r: \ \frac{\partial \hat{M}_{rr}}{\partial r} + \frac{1}{r}\frac{\partial \hat{M}_{r\theta}}{\partial \theta} + \frac{\hat{M}_{rr} - \hat{M}_{\theta\theta}}{r} - \hat{Q}_{rr} = 0 \qquad \delta \psi_\theta: \ \frac{\partial \hat{M}_{r\theta}}{\partial r} + \frac{1}{r}\frac{\partial \hat{M}_{\theta\theta}}{\partial \theta} + \frac{2\hat{M}_{r\theta}}{r} - \hat{Q}_{\theta\theta} = 0$$
$$\delta w: \ \frac{\partial \hat{Q}_{rr}}{\partial r} + \frac{1}{r}\frac{\partial \hat{Q}_{\theta\theta}}{\partial \theta} + \frac{\hat{Q}_{rr}}{r} + \frac{1}{r}\frac{\partial}{\partial r}\left(rN_{rr}\frac{\partial w}{\partial r}\right) + \frac{1}{r^2}\frac{\partial}{\partial \theta}\left(N_{\theta\theta}\frac{\partial w}{\partial \theta}\right) + \frac{2N_{r\theta}}{r}\frac{\partial^2 w}{\partial r \partial \theta}$$
$$+ \eta\left(\frac{\partial^2 (rP_{rr})}{r\partial r^2} + \frac{\partial^2 P_{\theta\theta}}{r^2 \partial \theta^2} - \frac{\partial P_{\theta\theta}}{r\partial r} + 2\frac{\partial^2 P_{r\theta}}{\partial r \partial \theta} + \frac{2}{r^2}\frac{\partial P_{r\theta}}{\partial \theta}\right) = 0 \tag{3}$$

Table 1. Comparison of Nondimensional Buckling Load of Sector Plates

		SSSS			SSCC			SSFF		
		Wang et al. (2000)			Wang et al. (2000)			Wang et al. (2000)		
β	h/b	Ritz	Analytical	Present	Ritz	Analytical	Present	Ritz	Analytical	Present
30°	0.001	96.92	—	97.252	122.90	—	122.903	35.77	—	—
	0.1	75.89	75.90	76.152	89.28	88.89	89.452	30.13	30.11	30.417
	0.2	45.97	45.98	46.368	49.72	49.24	50.375	22.61	22.54	23.200
45°	0.001	55.75	—	56.093	76.94	—	76.938	14.94	—	—
	0.1	48.08	48.09	48.350	62.10	62.05	62.159	13.53	13.54	13.663
	0.2	34.03	34.05	34.269	39.69	39.69	39.985	11.52	11.57	11.825
60°	0.001	38.85	—	39.205	57.82	—	57.582	7.73	—	—
	0.1	34.96	34.97	35.254	48.81	48.97	48.842	7.22	7.22	7.306
	0.2	26.88	26.90	27.104	33.70	33.88	33.866	6.51	6.50	6.698
90°	0.001	24.50	—	24.856	40.71	—	40.706	2.72	—	—
	0.1	22.89	22.90	23.204	36.12	36.10	36.134	2.61	2.61	2.671
	0.2	19.12	19.14	19.358	27.08	27.14	27.154	2.45	2.45	2.574
135°	0.001	16.44	—	16.415	31.00	—	30.864	—	—	—
	0.1	15.65	15.70	15.977	28.18	28.23	28.180	—	—	—
	0.2	13.78	13.84	14.049	22.37	22.41	22.403	—	—	—
180°	0.001	12.69	—	13.315	26.23	—	26.730	—	—	—
	0.1	12.23	12.25	12.659	24.24	24.21	24.404	—	—	—
	0.2	11.06	11.08	11.416	19.83	19.78	19.978	—	—	—

Table 2. Comparison among CPT, FSDT, and TSDT for Critical Buckling Load and Temperature of Thick, Annular Sector Plates versus the Variation of h/c and a/b for SSSS ($\beta = 60°$)

Type of loading	a/b	Theory	$h/c = 0.05$	$h/c = 0.1$	$h/c = 0.15$	$h/c = 0.2$	$h/c = 0.25$
N_{cr} (MN)	0.1	CPT	124.421	995.369	3359.372	7962.955	15552.647
		FSDT	121.646	912.263	2788.218	5837.714	9914.183
		TSDT	121.649	912.339	2789.331	5844.412	9938.758
	0.3	CPT	62.056	496.450	1675.518	3971.598	7757.028
		FSDT	61.154	468.818	1479.619	3215.626	5674.587
		TSDT	61.153	468.842	1479.900	3217.345	5681.301
	0.5	CPT	30.563	244.507	825.212	1956.060	3820.430
		FSDT	30.256	234.977	756.228	1683.205	3048.542
		TSDT	30.256	234.981	756.287	1683.657	3050.377
	0.7	CPT	14.445	115.562	390.022	924.497	1805.659
		FSDT	14.331	112.005	364.014	820.304	1506.644
		TSDT	14.332	112.007	364.033	820.439	1507.231
	0.9	CPT	4.340	34.720	117.181	277.763	542.506
		FSDT	4.309	33.758	110.115	249.321	460.434
		TSDT	4.309	33.758	110.120	249.355	460.582
T_{cr} (℃)	0.1	CPT	688.268	2753.070	6194.408	11012.280	17206.687
		FSDT	672.930	2523.232	5141.251	8073.202	10968.674
		TSDT	672.934	2523.462	5143.384	8082.524	10995.503
	0.3	CPT	441.360	1765.439	3972.238	7061.756	11033.993
		FSDT	434.944	1667.202	3507.794	5717.524	8071.809
		TSDT	434.945	1667.269	3508.449	5720.593	8081.310
	0.5	CPT	304.325	1217.300	2738.924	4869.198	7608.122
		FSDT	301.269	1169.854	2509.968	4189.987	6071.003
		TSDT	301.270	1169.876	2510.198	4191.118	6074.705
	0.7	CPT	239.728	958.909	2157.544	3835.633	5993.176
		FSDT	237.839	929.392	2013.658	3403.324	5000.695
		TSDT	237.839	929.403	2013.773	3403.904	5002.649
	0.9	CPT	216.077	864.306	1944.687	3457.221	5401.908
		FSDT	214.547	840.339	1827.423	3103.211	4584.695
		TSDT	214.547	840.347	1827.507	3103.642	4586.164

Also, the boundary conditions of the plate require

$$
\text{at } r = \text{const} \begin{cases} \text{either } \delta u = 0 & \text{or } N_{rr} = 0 \\ \text{either } \delta v = 0 & \text{or } N_{r\theta} = 0 \\ \text{either } \delta \phi_r = 0 & \text{or } \hat{M}_{rr} = 0 \\ \text{either } \delta \phi_\theta = 0 & \text{or } \hat{M}_{r\theta} = 0\theta \\ \text{either } \delta w = 0 & \text{or } \hat{Q}_{rr} + \eta \left(\dfrac{\partial P_{rr}}{\partial r} + \dfrac{2}{r} \dfrac{\partial P_{r\theta}}{\partial \theta} + \dfrac{P_{rr} - P_{\theta\theta}}{r} \right) = 0 \\ \text{either } \delta \frac{\partial w}{\partial r} = 0 & \text{or } P_{rr} = 0 \end{cases}
$$

$$
\text{at } \theta = \text{const} \begin{cases} \text{either } \delta u = 0 & \text{or } N_{r\theta} = 0 \\ \text{either } \delta v = 0 & \text{or } N_{\theta\theta} = 0 \\ \text{either } \delta \phi_r = 0 & \text{or } \hat{M}_{r\theta} = 0 \\ \text{either } \delta \phi_\theta = 0 & \text{or } \hat{M}_{\theta\theta} = 0 \\ \text{either } \delta w = 0 & \text{or } \hat{Q}_{\theta\theta} + \eta \left(\dfrac{\partial P_{\theta\theta}}{r \partial \theta} + 2 \dfrac{\partial P_{r\theta}}{\partial r} + \dfrac{2\alpha}{r} P_{r\theta} \right) = 0 \\ \text{either } \delta \frac{\partial w}{\partial \theta} = 0 & \text{or } P_{\theta\theta} = 0 \end{cases} \tag{4}
$$

Table 3. Comparison among CPT, FSDT, and TSDT for Critical Buckling Load and Temperature of Thick, Annular Sector Plates versus the Variation of h/c and a/b for SSCC ($\beta = 60°$)

Type of loading	a/b	Theory	$h/c = 0.05$	$h/c = 0.1$	$h/c = 0.15$	$h/c = 0.2$	$h/c = 0.25$
N_{cr} (MN)	0.1	CPT	184.207	1473.660	4973.603	11789.281	23025.940
		FSDT	177.222	1279.974	3728.554	7431.645	12071.267
		TSDT	177.243	1280.710	3734.890	7460.260	12157.677
	0.3	CPT	113.961	911.688	3076.946	7293.502	14245.120
		FSDT	109.958	799.550	2359.091	4786.104	7928.793
		TSDT	109.974	800.349	2365.375	4810.549	7994.067
	0.5	CPT	80.624	644.991	2176.844	5159.927	10077.982
		FSDT	78.163	573.415	1702.939	3462.663	5730.068
		TSDT	78.166	573.636	1705.258	3473.903	5765.002
	0.7	CPT	48.434(2)	387.478(2)	1307.740(2)	3099.828(2)	6054.351(2)
		FSDT	46.963(2)	344.616(2)	1023.563(2)	2081.036(2)	3442.652(2)
		TSDT	46.965(2)	344.736(2)	1024.872(2)	2087.478(2)	3462.985(2)
	0.9	CPT	16.136(7)	129.160(7)	435.916(7)	1033.283(7)	2018.131(7)
		FSDT	15.763(6)	114.832(7)	340.955(7)	692.968(7)	1146.045(7)
		TSDT	15.309(7)	112.469(7)	339.416(7)	679.054(7)	1132.643(7)
T_{cr} (℃)	0.1	CPT	1019.008	4076.032	9171.072	16304.127	25475.198
		FSDT	980.350	3540.282	6875.219	10277.479	13354.936
		TSDT	980.485	3542.320	6886.941	10317.227	13450.656
	0.3	CPT	810.525	3242.097	7294.717	12968.385	20263.102
		FSDT	782.056	2843.340	5592.838	8510.038	11278.282
		TSDT	782.178	2846.175	5607.784	8553.509	11371.227
	0.5	CPT	802.795	3211.178	7225.149	12844.710	20069.859
		FSDT	778.290	2854.830	5652.201	8619.694	11411.208
		TSDT	778.323	2855.921	5659.918	8647.621	11480.738
	0.7	CPT	803.801(2)	3215.201(2)	7234.203(2)	12860.804(2)	20095.006(2)
		FSDT	779.379(2)	2859.536(2)	5662.189(2)	8633.961(2)	11426.506(2)
		TSDT	779.408(2)	2860.534(2)	5669.435(2)	8660.683(2)	11493.999(2)
	0.9	CPT	803.337(7)	3213.347(7)	7234.268(7)	12860.921(7)	20095.188(7)
		FSDT	779.312(7)	2858.563(7)	5658.342(7)	8625.136(7)	11411.545(7)
		TSDT	779.341(7)	2802.041(7)	5665.646(7)	8652.105(7)	11479.710(7)

where the parameters $\hat{M}_{\xi\eta}$ and $\hat{Q}_{\xi\eta}$ are defined as

$$\hat{M}_{\xi\vartheta} = M_{\xi\vartheta} - \eta P_{\xi\vartheta} \qquad \hat{Q}_{\xi\vartheta} = Q_{\xi\vartheta} - \eta R_{\xi\vartheta} \qquad (\xi, \vartheta = r, \theta, z) \quad (5)$$

N_{rr}, $N_{\theta\theta}$, and $N_{r\theta}$ are the resultant forces; and M_{rr}, $M_{\theta\theta}$, and $M_{r\theta}$ are the resultant moments. Also, Q_{rr} and $Q_{\theta\theta}$ are the transverse shear forces; P_{rr}, $P_{\theta\theta}$, and $P_{r\theta}$ are the higher-order resultant moments; and R_{rr}, $R_{\theta\theta}$ are the higher-order shear forces. These parameters are defined as

$$\begin{aligned}
(N_{rr}, N_{\theta\theta}, N_{r\theta}) &= \int_{-h/2}^{h/2} (\sigma_{rr}, \sigma_{\theta\theta}, \sigma_{r\theta}) dz \\
(M_{rr}, M_{\theta\theta}, M_{r\theta}) &= \int_{-h/2}^{h/2} (\sigma_{rr}, \sigma_{\theta\theta}, \sigma_{r\theta}) z dz \\
(P_{rr}, P_{\theta\theta}, P_{r\theta}) &= \int_{-h/2}^{h/2} (\sigma_{rr}, \sigma_{\theta\theta}, \sigma_{r\theta}) z^3 dz \\
(Q_{rr}, Q_{\theta\theta}) &= \int_{-h/2}^{h/2} (\sigma_{rz}, \sigma_{\theta z}) dz \\
(R_{rr}, R_{\theta\theta}) &= \int_{-h/2}^{h/2} (\sigma_{rz}, \sigma_{\theta z}) z^2 dz
\end{aligned} \quad (6)$$

where σ_{rr} and $\sigma_{\theta\theta}$ are the normal stresses, and $\sigma_{r\theta}$, $\sigma_{\theta\theta}$, and $\sigma_{\theta z}$ are the shear stresses. Based on the Hooke's law and considering the thermal effects, the following stress-strain relations can be written as follows:

$$\begin{aligned}
\sigma_{rr} &= \frac{E}{1-\nu^2}[\varepsilon_{rr} + \nu\varepsilon_{\theta\theta} - (1+\nu)\alpha T(r,\theta,z)] \\
\sigma_{\theta\theta} &= \frac{E}{1-\nu^2}[\varepsilon_{\theta\theta} + \nu\varepsilon_{rr} - (1+\nu)\alpha T(r,\theta,z)] \\
\sigma_{r\theta} &= \frac{E}{2(1+\nu)}(2\varepsilon_{r\theta}) \qquad \sigma_{\theta z} = \frac{E}{2(1+\nu)}(2\varepsilon_{\theta z}) \\
\sigma_{rz} &= \frac{E}{2(1+\nu)}(2\varepsilon_{rz})
\end{aligned} \quad (7)$$

where α is the coefficient of thermal expansion, ν is the Poisson ratio, and $T(r, \theta, z)$ is the temperature profile.

Stability Equations

The stability equations of the plate can be derived from the adjacent equilibrium criterion (Brush and Almroth 1975). It is assumed that the plate whose stability is under investigation is in the equilibrium

Table 4. Comparison among CPT, FSDT, and TSDT for Critical Buckling Load and Temperature of Thick, Annular Sector Plates versus the Variation of h/c and a/b for SSFF ($\beta = 60°$)

Type of loading	a/b	Theory	$h/c = 0.05$	$h/c = 0.1$	$h/c = 0.15$	$h/c = 0.2$	$h/c = 0.25$
N_{cr} (MN)	0.1	CPT	23.763	190.109	641.617	1520.870	2970.450
		FSDT	23.316	181.509	591.445	1344.714	2504.707
		TSDT	23.954	186.557	608.654	1385.709	2585.567
	0.3	CPT	10.985	87.884	296.608	703.072	1373.188
		FSDT	10.818	84.793	279.045	642.151	1212.799
		TSDT	11.120	87.132	286.980	661.058	1250.099
	0.5	CPT	3.682	29.457	99.417	235.656	460.265
		FSDT	3.634	28.617	94.807	220.031	419.757
		TSDT	3.752	29.391	97.450	226.399	432.331
	0.7	CPT	0.682	5.454	18.408	43.633	85.221
		FSDT	0.674	5.322	17.704	41.310	79.305
		TSDT	0.742	5.476	18.195	42.491	81.654
	0.9	CPT	0.209	0.167	0.564	1.337	2.611
		FSDT	0.207	0.163	0.544	1.273	2.451
		TSDT	0.534	0.224	0.603	1.335	2.540
T_{cr} (°C)	0.1	CPT	131.443	525.770	1182.981	2103.077	3286.058
		FSDT	128.979	501.978	1090.568	1859.532	2770.891
		TSDT	132.492	515.947	1122.201	1916.208	2860.255
	0.3	CPT	78.123	312.491	703.103	1249.961	1953.063
		FSDT	76.939	301.529	661.531	1141.717	1725.014
		TSDT	79.083	309.820	680.310	1175.375	1778.070
	0.5	CPT	36.662	146.647	329.955	586.586	916.540
		FSDT	36.186	142.465	314.661	547.718	835.885
		TSDT	37.353	146.331	323.428	563.515	860.919
	0.7	CPT	11.313	45.252	101.817	181.008	282.825
		FSDT	11.183	44.156	97.935	171.377	263.192
		TSDT	12.309	45.434	100.652	176.264	270.971
	0.9	CPT	1.041	4.161	9.361	16.642	26.003
		FSDT	1.029	4.068	9.039	15.853	24.411
		TSDT	—	5.572	9.999	16.616	25.294

configuration (u^0, v^0, w^0, ϕ_r^0, ϕ_θ^0). The displacement components of a neighboring configuration of the stable state can be expressed as follows:

$$u = u^0 + u^1 \qquad v = v^0 + v^1 \qquad w = w^0 + w^1$$
$$\phi_r = \phi_r^0 + \phi_r^1 \qquad \phi_\theta = \phi_\theta^0 + \phi_\theta^1 \tag{8}$$

where u^1, v^1, w^1, ϕ_r^1, and ϕ_θ^1 are infinitesimally small increments from the stable configuration. Similarly, the force and moment resultants in a neighboring state can be expressed as

$$N_{rr} = N_{rr}^0 + N_{rr}^1 \qquad N_{\theta\theta} = N_{\theta\theta}^0 + N_{\theta\theta}^1 \qquad N_{r\theta} = N_{r\theta}^0 + N_{r\theta}^1$$
$$M_{rr} = M_{rr}^0 + M_{rr}^1 \qquad M_{\theta\theta} = M_{\theta\theta}^0 + M_{\theta\theta}^1 \qquad M_{r\theta} = M_{r\theta}^0 + M_{r\theta}^1$$
$$Q_{rr} = Q_{rr}^0 + Q_{rr}^1 \qquad Q_{\theta\theta} = Q_{\theta\theta}^0 + Q_{\theta\theta}^1 \qquad P_{rr} = P_{rr}^0 + P_{rr}^1$$
$$P_{\theta\theta} = P_{\theta\theta}^0 + P_{\theta\theta}^1 \qquad P_{r\theta} = P_{r\theta}^0 + P_{r\theta}^1 \qquad R_{rr} = R_{rr}^0 + R_{rr}^1$$
$$R_{\theta\theta} = R_{\theta\theta}^0 + R_{\theta\theta}^1 \tag{9}$$

where the terms with subscript 0 correspond to (u^0, v^0, w^0, ϕ_r^0, ϕ_θ^0), and the terms with the subscripts 1 are variations in the force and moment resultants corresponding to the u^1, v^1, w^1, ϕ_r^1, and ϕ_θ^1. Substituting relations (8) into the equilibrium equations and eliminating quadratic and cubic incremental terms yields the stability equations of annular sector plate as

$$\frac{\partial N_{rr}^1}{\partial r} + \frac{1}{r}\frac{\partial N_{r\theta}^1}{\partial \theta} + \frac{N_{rr}^1 - N_{\theta\theta}^1}{r} = 0$$
$$\frac{\partial N_{r\theta}^1}{\partial r} + \frac{1}{r}\frac{\partial N_{\theta\theta}^1}{\partial \theta} + \frac{2N_{r\theta}^1}{r} = 0$$
$$\frac{\partial \hat{M}_{rr}^1}{\partial r} + \frac{1}{r}\frac{\partial \hat{M}_{r\theta}^1}{\partial \theta} + \frac{\hat{M}_{rr}^1 - \hat{M}_{\theta\theta}^1}{r} - \hat{Q}_{rr}^1 = 0$$
$$\frac{\partial \hat{M}_{r\theta}^1}{\partial r} + \frac{1}{r}\frac{\partial \hat{M}_{\theta\theta}^1}{\partial \theta} + \frac{2\hat{M}_{r\theta}^1}{r} - \hat{Q}_{\theta\theta}^1 = 0$$
$$\frac{\partial \hat{Q}_{rr}^1}{\partial r} + \frac{1}{r}\frac{\partial \hat{Q}_{\theta\theta}^1}{\partial \theta} + \frac{\hat{Q}_{rr}^1}{r} + + \frac{1}{r}\frac{\partial}{\partial r}\left(rN_{rr}^0\frac{\partial w^1}{\partial r}\right)$$
$$+ \frac{1}{r^2}\frac{\partial}{\partial \theta}\left(N_{\theta\theta}^0\frac{\partial w^1}{\partial \theta}\right) + \frac{2N_{r\theta}^0}{r}\frac{\partial^2 w^1}{\partial r \partial \theta}$$
$$+ \eta\left(\frac{\partial^2 (rP_{rr}^1)}{r\partial r^2} + \frac{\partial^2 P_{\theta\theta}^1}{r^2\partial\theta^2} - \frac{\partial P_{\theta\theta}^1}{r\partial r} + 2\frac{\partial^2 P_{r\theta}^1}{\partial r\partial\theta} + \frac{2}{r^2}\frac{\partial P_{r\theta}^1}{\partial\theta}\right) = 0 \tag{10}$$

Substituting Eqs. (2) and (7) into Eq. (6) gives the following relations for force and moment resultants

Table 5. Comparison among CPT, FSDT, and TSDT for Critical Buckling Load and Temperature of Thick, Annular Sector Plates versus the Variation of h/c and a/b for SSSF ($\beta = 60°$)

Type of loading	a/b	Theory	$h/c = 0.05$	$h/c = 0.1$	$h/c = 0.15$	$h/c = 0.2$	$h/c = 0.25$
N_{cr} (MN)	0.1	CPT	23.773	190.185	641.874	1521.479	2971.639
		FSDT	23.329	181.585	591.788	1345.526	2506.292
		TSDT	23.963	186.658	608.997	1386.521	2587.153
	0.3	CPT	11.342	90.737	306.236	725.893	1417.761
		FSDT	11.181	87.705	288.834	665.068	1256.813
		TSDT	11.488	90.080	296.890	684.261	1294.485
	0.5	CPT	4.488	35.908	121.188	287.262	561.058
		FSDT	4.438	35.003	116.138	269.932	515.793
		TSDT	4.568	35.855	119.001	276.753	529.114
	0.7	CPT	1.179	9.433	31.837	75.465	147.393
		FSDT	1.166	9.218	30.699	71.722	137.939
		TSDT	1.241	9.381	31.212	72.932	140.317
	0.9	CPT	0.054	0.437	1.476	3.498	6.832
		FSDT	0.053	0.426	1.417	3.314	6.381
		TSDT	—	0.477	1.447	3.344	6.424
T_{cr} (℃)	0.1	CPT	131.500	526.000	1183.499	2103.998	3287.496
		FSDT	129.044	502.251	1091.194	1860.635	2772.569
		TSDT	132.558	516.222	1122.828	1917.311	2861.930
	0.3	CPT	80.659	322.636	725.930	1290.543	2016.472
		FSDT	79.518	311.893	684.739	1182.497	1787.688
		TSDT	81.708	320.336	703.804	1216.568	1841.249
	0.5	CPT	44.693	178.770	402.232	715.079	1117.310
		FSDT	44.192	174.263	385.463	671.946	1027.074
		TSDT	45.483	178.492	394.951	688.866	1053.620
	0.7	CPT	19.568	78.269	176.105	313.075	489.180
		FSDT	19.355	76.484	169.812	297.566	457.822
		TSDT	20.595	77.841	172.648	302.584	465.683
	0.9	CPT	2.721	10.884	24.489	43.536	68.025
		FSDT	2.686	10.600	23.525	41.242	63.529
		TSDT	—	11.873	24.011	41.620	63.965

$$N^1_{rr} = A\left[\frac{\partial u^1}{\partial r} + \nu\left(\frac{1}{r}\frac{\partial v^1}{\partial \theta} + \frac{u^1}{r}\right)\right] - \frac{T_N}{1-\nu} \qquad N^1_{\theta\theta} = A\left[\left(\frac{1}{r}\frac{\partial v^1}{\partial \theta} + \frac{u^1}{r}\right) + \nu\frac{\partial u^1}{\partial r}\right] - \frac{T_N}{1-\nu} \qquad N^1_{r\theta} = \frac{A(1-\nu)}{2}\left(\frac{1}{r}\frac{\partial u^1}{\partial \theta} + \frac{\partial v^1}{\partial r} - \frac{v^1}{r}\right)$$

$$M^1_{rr} = D\left[\frac{\partial \phi^1_r}{\partial r} + \nu\left(\frac{1}{r}\frac{\partial \phi^1_\theta}{\partial \theta} + \frac{\phi^1_r}{r}\right)\right] - \eta H\left[\left(\frac{\partial \phi^1_r}{r} + \frac{\partial^2 w^1}{\partial r^2}\right) + \nu\left(\frac{1}{r}\frac{\partial \phi^1_\theta}{\partial \theta} + \frac{\phi^1_r}{r} + \frac{1}{r^2}\frac{\partial^2 w^1}{\partial \theta^2} + \frac{1}{r}\frac{\partial w^1}{\partial r}\right)\right] - \frac{T_M}{1-\nu}$$

$$M^1_{\theta\theta} = D\left[\left(\frac{1}{r}\frac{\partial \phi^1_\theta}{\partial \theta} + \frac{\phi^1_r}{r}\right) + \nu\frac{\partial \phi^1_r}{\partial r}\right] - \eta H\left[\left(\frac{1}{r}\frac{\partial \phi^1_\theta}{\partial \theta} + \frac{\phi^1_r}{r} + \frac{1}{r^2}\frac{\partial^2 w^1}{\partial \theta^2} + \frac{1}{r}\frac{\partial w^1}{\partial r}\right) + \nu\left(\frac{\partial \phi^1_r}{r} + \frac{\partial^2 w^1}{\partial r^2}\right)\right] - \frac{T_M}{1-\nu}$$

$$M^1_{r\theta} = \frac{D(1-\nu)}{2}\left(\frac{1}{r}\frac{\partial \phi^1_r}{\partial \theta} + \frac{\partial \phi^1_\theta}{\partial r} - \frac{\phi^1_\theta}{r}\right) - \frac{\eta H(1-\nu)}{2}\left(\frac{1}{r}\frac{\partial \phi^1_v}{\partial \theta} + \frac{\partial \phi^1_\theta}{\partial r} - \frac{\phi^1_\theta}{r} + \frac{2}{r}\frac{\partial^2 w^1}{\partial r \partial \theta} - \frac{2}{r^2}\frac{\partial w^1}{\partial \theta}\right)$$

$$P^1_{rr} = H\left[\frac{\partial \phi^1_r}{\partial r} + \nu\left(\frac{1}{r}\frac{\partial \phi^1_\theta}{\partial \theta} + \frac{\phi^1_r}{r}\right)\right] - \eta F\left[\left(\frac{\partial \phi^1_r}{r} + \frac{\partial^2 w^1}{\partial r^2}\right) + \nu\left(\frac{1}{r}\frac{\partial \phi^1_\theta}{\partial \theta} + \frac{\phi^1_r}{r} + \frac{1}{r^2}\frac{\partial^2 w^1}{\partial \theta^2} + \frac{1}{r}\frac{\partial w^1}{\partial r}\right)\right] - \frac{T_P}{1-\nu}$$

$$P^1_{\theta\theta} = H\left[\left(\frac{1}{r}\frac{\partial \phi^1_\theta}{\partial \theta} + \frac{\phi^1_r}{r}\right) + \nu\frac{\partial \phi^1_r}{\partial r}\right] - \eta F\left[\left(\frac{1}{r}\frac{\partial \phi^1_\theta}{\partial \theta} + \frac{\phi^1_r}{r} + \frac{1}{r^2}\frac{\partial^2 w^1}{\partial \theta^2} + \frac{1}{r}\frac{\partial w^1}{\partial r}\right) + \nu\left(\frac{\partial \phi^1_r}{r} + \frac{\partial^2 w^1}{\partial r^2}\right)\right] - \frac{T_P}{1-\nu}$$

$$P^1_{r\theta} = \frac{H(1-\nu)}{2}\left(\frac{1}{r}\frac{\partial \phi^1_r}{\partial \theta} + \frac{\partial \phi^1_\theta}{\partial r} - \frac{\phi^1_\theta}{r}\right) - \frac{\eta F(1-\nu)}{2}\left(\frac{1}{r}\frac{\partial \phi^1_r}{\partial \theta} + \frac{\partial \phi^1_\theta}{\partial r} - \frac{\phi^1_\theta}{r} + \frac{2}{r}\frac{\partial^2 w^1}{\partial r \partial \theta} - \frac{2}{r^2}\frac{\partial w^1}{\partial \theta}\right) \qquad Q^1_{rr} = \frac{(1-\nu)(A-3\eta D)}{2}\left(\phi^1_r + \frac{\partial w^1}{\partial r}\right)$$

$$Q^1_{\theta\theta} = \frac{(1-\nu)(A-3\eta D)}{2}\left(\phi^1_\theta + \frac{1}{r}\frac{\partial w^1}{\partial \theta}\right) \qquad R^1_{rr} = \frac{(1-\nu)(D-3\eta H)}{2}\left(\phi^1_r + \frac{\partial w^1}{\partial r}\right) \qquad R^1_{\theta\theta} = \frac{(1-\nu)(D-3\eta H)}{2}\left(\phi^1_\theta + \frac{1}{r}\frac{\partial w^1}{\partial \theta}\right) \tag{11}$$

Table 6. Comparison among CPT, FSDT, and TSDT for Critical Buckling Load and Temperature of Thick, Annular Sector Plates versus the Variation of h/c and a/b for SSCF ($\beta = 60°$)

Type of loading	a/b	Theory	$h/c = 0.05$	$h/c = 0.1$	$h/c = 0.15$	$h/c = 0.2$	$h/c = 0.25$
N_{cr} (MN)	0.1	CPT	23.798	190.387	642.559	1523.103	2974.810
		FSDT	23.345	181.661	599.322	1420.615	2774.639
		TSDT	23.979	186.735	609.168	1386.926	2587.549
	0.3	CPT	12.152	97.218	328.110	777.743	1519.029
		FSDT	11.936	92.945	303.658	694.287	1305.488
		TSDT	12.246	95.356	311.916	714.149	1343.721
	0.5	CPT	6.659	12.248	179.808	426.212	832.446
		FSDT	6.555	11.764	167.374	382.575	717.992
		TSDT	6.682	11.958	170.266	389.639	732.196
	0.7	CPT	3.561	28.487	96.145	227.899	445.117
		FSDT	3.525	27.764	91.833	212.423	403.394
		TSDT	3.591	27.910	92.298	213.558	405.684
	0.9	CPT	1.084	8.674	29.276	69.396	135.539
		FSDT	1.081	8.588	28.688	67.080	128.822
		TSDT	—	8.630	28.713	67.107	128.865
T_{cr} (℃)	0.1	CPT	131.634	526.536	1184.706	2106.144	3290.850
		FSDT	129.128	502.454	1091.521	1861.099	2773.181
		TSDT	132.645	516.437	1123.180	1917.813	2862.597
	0.3	CPT	86.428	345.712	777.852	1382.848	2160.699
		FSDT	84.888	330.519	719.889	1234.461	1855.537
		TSDT	87.092	339.089	739.453	1269.737	1911.301
	0.5	CPT	66.312	265.246	596.804	1060.984	1657.788
		FSDT	65.268	254.753	555.520	952.295	1429.726
		TSDT	66.535	258.948	565.118	969.869	1458.124
	0.7	CPT	59.095	236.380	531.854	945.519	1477.372
		FSDT	58.492	230.379	507.992	881.319	1338.909
		TSDT	59.589	231.596	510.581	886.010	1346.487
	0.9	CPT	53.985	215.938	485.860	863.751	1349.611
		FSDT	53.812	213.791	476.105	834.922	1282.722
		TSDT	—	214.825	476.509	835.257	1283.148

where the parameters A, D, F, and H are the material stiffness coefficients of the plate which are as follows:

$$A = \frac{Eh}{1-\nu^2} \qquad D = \frac{Eh^3}{12(1-\nu^2)} \qquad H = \frac{Eh^5}{80(1-\nu^2)} \qquad F = \frac{Eh^7}{448(1-\nu^2)} \tag{12}$$

Also, the parameter T_N, T_M, and T_P are defined as

$$T_N = \int_{-h/2}^{h/2} E\alpha T(r,\theta,z)dz = Th\alpha E \qquad T_M = \int_{-h/2}^{h/2} E\alpha z T(r,\theta,z)dz = 0 \qquad T_P = \int_{-h/2}^{h/2} E\alpha z^2 T(r,\theta,z)dz = \frac{1}{12}Th^3\alpha E \tag{13}$$

Substituting resultants forces and moments obtained from Eqs. (10) and (11), yields the governing stability equations as

$$\begin{aligned}
&\xi\left[\left(\frac{\partial^2\phi_r^1}{\partial r^2}+\frac{1}{r}\frac{\partial\phi_r^1}{\partial r}-\frac{1}{r^2}\frac{\partial_\theta^1}{\partial\theta}-\frac{\phi_r^1}{r^2}+\frac{1}{r}\frac{\partial^2\phi_\theta}{\partial r\partial\theta}\right)+\frac{1-\nu}{2}\left(\frac{1}{r^2}\frac{\partial^2\phi_r^1}{\partial\theta^2}-\frac{1}{r}\frac{\partial^2\phi_\theta^1}{\partial r\partial\theta}-\frac{1}{r^2}\frac{\partial\phi_\theta^1}{\partial\theta}\right)\right]\\
&-\eta\Phi\left[\left(\frac{\partial^2\phi_r^1}{\partial r^2}+\frac{1}{r}\frac{\partial\phi_r^1}{\partial r}-\frac{1}{r^2}\frac{\partial\phi_\theta^1}{\partial\theta}-\frac{\phi_r^1}{r^2}+\frac{\partial^3 w^1}{\partial r^3}+\frac{1}{r}\frac{\partial^2 w^1}{\partial r^2}-\frac{2}{r^3}\frac{\partial^2 w^1}{\partial\theta^2}+\frac{1}{r}\frac{\partial^2\phi_\theta^1}{\partial r\partial\theta}+\frac{1}{r^2}\frac{\partial^3 w^1}{\partial r\partial\theta^2}-\frac{1}{r^2}\frac{\partial w^1}{\partial r}\right)\right.\\
&\left.+\frac{1-\nu}{2}\left(\frac{1}{r^2}\frac{\partial^2\phi_r^1}{\partial\theta^2}-\frac{1}{r}\frac{\partial^2\phi_\theta^1}{\partial r\partial\theta}-\frac{1}{r^2}\frac{\partial\phi^1}{\partial\theta}\right)\right]-\Gamma\left(\phi_r^1+\frac{\partial w^1}{\partial r}\right)=0
\end{aligned} \tag{14a}$$

Table 7. Comparison among CPT, FSDT, and TSDT for Critical Buckling Load and Temperature of Thick, Annular Sector Plates versus the Variation of h/c and a/b for SSFS ($\beta = 60°$)

Type of loading	a/b	Theory	$h/c = 0.05$	$h/c = 0.1$	$h/c = 0.15$	$h/c = 0.2$	$h/c = 0.25$
N_{cr} (MN)	0.1	CPT	124.190	993.517	3353.122	7948.140	15523.711
		FSDT	121.396	910.310	2782.395	5826.349	9896.742
		TSDT	121.393	910.386	2783.509	5833.047	9920.921
	0.3	CPT	56.755	454.041	1532.390	3632.332	7094.399
		FSDT	55.955	430.253	1364.568	2983.879	5301.030
		TSDT	55.836	429.418	1362.111	2979.200	5295.249
	0.5	CPT	19.901	159.207	537.326	1273.661	2487.619
		FSDT	19.641	153.061	497.159	1121.974	2067.250
		TSDT	19.369	151.225	490.803	1106.489	2036.326
	0.7	CPT	3.173	25.386	85.677	203.088	396.656
		FSDT	3.104	24.212	79.421	182.448	344.452
		TSDT	2.958	23.900	78.460	180.215	340.150
	0.9	CPT	0.075	0.603	2.034	4.822	9.418
		FSDT	0.074	0.582	1.930	4.491	8.605
		TSDT	—	0.519	1.895	4.456	8.559
T_{cr} (℃)	0.1	CPT	686.998	2747.990	6182.977	10991.960	17174.936
		FSDT	671.528	2517.792	5130.455	8057.425	10949.336
		TSDT	671.520	2518.009	5132.605	8066.783	10976.120
	0.3	CPT	403.661	1614.642	3632.944	6458.566	10091.509
		FSDT	397.971	1530.031	3235.072	5305.484	7540.355
		TSDT	397.127	1527.054	3229.218	5297.296	7532.300
	0.5	CPT	198.160	792.637	1783.433	3170.547	4953.979
		FSDT	195.570	762.028	1650.093	2792.960	4116.818
		TSDT	192.865	752.899	1628.983	2754.372	4055.196
	0.7	CPT	52.662	210.647	473.955	842.587	1316.542
		FSDT	51.516	200.904	439.343	756.950	1143.242
		TSDT	49.097	198.314	434.015	747.678	1128.973
	0.9	CPT	3.752	15.006	33.762	60.021	93.782
		FSDT	3.688	14.495	32.029	55.894	85.684
		TSDT	—	12.930	31.447	55.468	85.227

$$\xi\left[\left(\frac{1}{r^2}\frac{\partial^2\phi_\theta^1}{\partial\theta^2}+\frac{1}{r}\frac{\partial^2\phi_r^1}{\partial r\partial\theta}+\frac{1}{r^2}\frac{\partial\phi_r^1}{\partial\theta}\right)++\frac{1-\nu}{2}\left(\frac{\partial^2\phi_\theta^1}{\partial r^2}+\frac{1}{r}\frac{\partial\phi_\theta^1}{\partial r}+\frac{1}{r^2}\frac{\partial\phi_r^1}{\partial\theta}-\frac{\phi_\theta^1}{r^2}-\frac{1}{r}\frac{\partial^2\phi_r}{\partial r\partial\theta}\right)\right]$$
$$-\eta\Phi\left[\left(\frac{1}{r^2}\frac{\partial^2\phi_\theta^1}{\partial\theta^2}+\frac{1}{r}\frac{\partial^2\phi_r^1}{\partial r\partial\theta}+\frac{1}{r^2}\frac{\partial\phi_r^1}{\partial\theta}+\frac{1}{r^3}\frac{\partial^3w^1}{\partial\theta^3}+\frac{1}{r^2}\frac{\partial^2w^1}{\partial r\partial\theta}+\frac{1}{r^2}\frac{\partial^3w^1}{\partial r^2\partial\theta}\right)+\frac{1-\nu}{2}\left(\frac{\partial^2\phi_r^1}{\partial r^2}-\frac{1}{r}\frac{\partial\phi_\theta^1}{\partial r\partial\theta}+\frac{1}{r^2}\frac{\partial\phi_r^1}{\partial\theta}+\frac{1}{r}\frac{\partial\phi_\theta^1}{\partial r}-\frac{\phi_\theta^1}{r^2}\right)\right] \quad (14b)$$
$$-\Gamma\left(\phi_\theta^1+\frac{1}{r}\frac{\partial w^1}{\partial\theta}\right)=0$$

$$\Gamma\left(\frac{\partial\phi_{rr}^1}{\partial r}+\frac{1}{r}\frac{\partial\phi_{\theta\theta}^1}{\partial\theta}+\frac{\phi_{rr}^1}{r}+\frac{\partial^2w^1}{\partial r^2}+\frac{1}{r}\frac{\partial w^1}{\partial r}+\frac{1}{r^2}\frac{\partial^2w^1}{\partial\theta^2}\right)+\frac{1}{r}\frac{\partial}{\partial r}\left(rN_{rr}^0\frac{\partial w^1}{\partial r}\right)+\frac{1}{r^2}\frac{\partial}{\partial\theta}\left(N_{\theta\theta}^0\frac{\partial w^1}{\partial\theta}\right)+\frac{2N_{r\theta}^0}{r}\frac{\partial^2w^1}{\partial r\partial\theta}$$
$$+(\eta H-\eta^2F)\left(\frac{\partial^3\phi_r^1}{\partial r^3}+\frac{2}{r}\frac{\partial^2\phi_r^1}{\partial r^2}-\frac{1}{r^2}\frac{\partial\phi_r^1}{\partial r}+\frac{\phi_r^1}{r^3}+\frac{1}{r^3}\frac{\partial\phi_\theta^1}{\partial\theta}-\frac{1}{r^2}\frac{\partial^2\phi_\theta^1}{\partial r\partial\theta}+\frac{1}{r}\frac{\partial^3\phi_\theta^1}{\partial r^2\partial\theta}+\frac{1}{r^2}\frac{\partial^2\phi_r^1}{\partial r\partial\theta^2}+\frac{1}{r^3}\frac{\partial^2\phi_r^1}{\partial\theta^2}+\frac{1}{r^3}\frac{\partial^3\phi_\theta^1}{\partial\theta^3}\right) \quad (14c)$$
$$-\eta^2F\left(\frac{\partial^4w^1}{\partial r^4}+\frac{2}{r}\frac{\partial^3w^1}{\partial r^3}-\frac{1}{r^2}\frac{\partial^2w^1}{\partial r^2}+\frac{1}{r^3}\frac{\partial w^1}{\partial r}+\frac{2}{r^2}\frac{\partial^4w^1}{\partial r^2\partial\theta^2}-\frac{2}{r^3}\frac{\partial^3w^1}{\partial r\partial\theta^2}+\frac{4}{r^4}\frac{\partial^2w^1}{\partial\theta^2}+\frac{1}{r^4}\frac{\partial^4w^1}{\partial\theta^4}\right)=0$$

where the parameters Φ and ξ are defined as

$$\xi=D-\eta H \qquad \Phi=H-\eta F \quad (15)$$

Table 8. Comparison among CPT, FSDT, and TSDT for Critical Buckling Load and Temperature of Thick, Annular Sector Plates versus the Variation of h/c and a/b for SSFC ($\beta=60°$)

Type of loading	a/b	Theory	$h/c=0.05$	$h/c=0.1$	$h/c=0.15$	$h/c=0.2$	$h/c=0.25$
N_{cr} (MN)	0.1	CPT	182.248	1457.983	4920.691	11663.861	22780.979
		FSDT	175.719	1271.628	3708.691	7398.768	12026.476
		TSDT	175.722	1272.136	3714.342	7425.759	12110.112
	0.3	CPT	83.169	665.355	2245.572	5322.837	10396.167
		FSDT	81.391	612.359	1881.448	3965.678	6785.931
		TSDT	81.089	610.258	1875.728	3956.893	6780.709
	0.5	CPT	28.258	226.064	762.967	1808.515	3532.255
		FSDT	27.363	208.295	659.263	1448.837	2601.462
		TSDT	26.916	205.372	649.515	1426.113	2558.236
	0.7	CPT	6.056	48.446	163.507	387.572	756.977
		FSDT	5.919	46.033	150.259	342.947	642.498
		TSDT	5.777	45.734	149.355	340.895	638.637
	0.9	CPT	1.141	9.127	30.804	73.016	142.610
		FSDT	1.136	9.022	30.110	70.334	134.930
		TSDT	0.934	8.969	30.082	70.309	134.900
T_{cr} (℃)	0.1	CPT	1008.163	4032.649	9073.460	16130.595	25204.055
		FSDT	972.048	3517.214	6838.581	10231.970	13305.606
		TSDT	972.053	3518.613	6848.991	10269.538	13397.838
	0.3	CPT	591.525	2366.098	5323.720	9464.391	14788.110
		FSDT	578.879	2177.664	4460.513	7051.277	9652.689
		TSDT	576.736	2170.184	4446.893	7035.714	9645.340
	0.5	CPT	281.373	1125.492	2532.356	4501.966	7034.322
		FSDT	272.460	1037.016	2188.130	3606.561	5180.606
		TSDT	268.010	1022.473	2155.800	3550.032	5094.545
	0.7	CPT	100.499	401.993	904.483	1607.969	2512.451
		FSDT	98.238	381.966	831.204	1422.847	2132.503
		TSDT	95.884	379.495	826.209	1414.318	2119.670
	0.9	CPT	56.801	227.203	511.206	908.811	1420.017
		FSDT	56.577	224.589	499.696	875.427	1343.534
		TSDT	46.490	223.284	499.222	875.109	1343.242

Eqs. (14*a*) and (14*b*) are three highly coupled partial differential equations. For solving these equations, it is reasonable to find a method for decoupling them. Using the following analytical method, these coupled stability equations are decoupled.

Decoupling the Equations

Eqs. (14*a*) and (14*b*) can be rewritten as

$$X\left[\frac{\partial\Psi_1}{\partial r}+\frac{1-\nu}{2}\left(\frac{1}{r}\frac{\partial\Psi_2}{\partial\theta}\right)\right]-\eta\Phi\frac{\partial}{\partial r}(\nabla^2 w^1)-\Gamma\left(\phi_r^1+\frac{\partial w^1}{\partial r}\right)=0 \tag{16a}$$

$$X\left[\left(\frac{1}{r}\frac{\partial\Psi_1}{\partial\theta}\right)+\frac{1-\nu}{2}\frac{\partial\Psi_2}{\partial r}\right]-\eta\Phi\frac{1}{r}\frac{\partial}{\partial\theta}(\nabla^2 w^1)-\Gamma\left(\phi_\theta^1+\frac{1}{r}\frac{\partial w^1}{\partial\theta}\right)=0 \tag{16b}$$

$$\Gamma\left(\Psi_1+\nabla^2 w^1\right)+\frac{1}{r}\frac{\partial}{\partial r}\left(rN_{rr}^0\frac{\partial w^1}{\partial r}\right)+\frac{1}{r^2}\frac{\partial}{\partial\theta}\left(N_{\theta\theta}^0\frac{\partial w^1}{\partial\theta}\right)+\frac{2N_{r\theta}^0}{r}\frac{\partial^2 w^1}{\partial r\partial\theta}+\eta\Phi\nabla^2\Psi_1-\eta^2F\nabla^4 w^1=0 \tag{16c}$$

where ∇^2 is the Laplacian operator in polar coordinates and $\nabla^4=\nabla^2(\nabla^2)$. Also, the parameters Ψ_1, $\Psi_2 X$, and Γ are defined as

$$\Psi_1=\frac{\partial\phi_r^1}{\partial r}+\frac{\phi_r^1}{r}+\frac{1}{r}\frac{\partial\phi_\theta^1}{\partial\theta}\qquad \Psi_2=\frac{1}{r}\frac{\partial\phi_r^1}{\partial\theta}-\frac{\partial\phi_\theta^1}{\partial r}-\frac{\phi_\theta^1}{r}$$
$$X=\xi-\eta\Phi\qquad \Gamma=\frac{1-\nu}{2}(A-6\eta D+9\eta^2 H) \tag{17}$$

By differentiating Eqs. (16*a*) and (16*b*) with respect to r and θ doing some algebraic operations, it is easy to show that

$$X\nabla^2\Psi_1-\eta\Phi\nabla^4 w^1-\Gamma(\Psi_1+\nabla^2 w^1)=0 \tag{18a}$$

$$\frac{X(1-\nu)}{2}\nabla^2\Psi_2-\Gamma\Psi_2=0 \tag{18b}$$

By considering Eqs. (16*c*) and (18*a*) and doing some algebraic operations, the parameters Ψ_1 can be obtained as

$$\Psi_1=\left(\frac{\eta^2FX-\eta^2\Phi^2}{\Gamma(X+\eta\Phi)}\right)\nabla^4 w^1-\nabla^2 w^1-\frac{X}{\Gamma(X+\eta\Phi)}\left[\frac{1}{r}\frac{\partial}{\partial r}\left(rN_{rr}^0\frac{\partial w^1}{\partial r}\right)+\frac{1}{r^2}\frac{\partial}{\partial\theta}\left(N_{\theta\theta}^0\frac{\partial w^1}{\partial\theta}\right)+\frac{2N_{r\theta}^0}{r}\frac{\partial^2 w^1}{\partial r\partial\theta}\right] \tag{19}$$

Table 9. Comparison among CPT, FSDT, and TSDT for Critical Buckling Load and Temperature of Thick, Annular Sector Plates versus the Variation of h/c and a/b for SSSC ($\beta=60°$)

Type of loading	a/b	Theory	$h/c=0.05$	$h/c=0.1$	$h/c=0.15$	$h/c=0.2$	$h/c=0.25$
N_{cr} (MN)	0.1	CPT	182.885	1463.082	4937.900	11704.653	22860.650
		FSDT	176.400	1276.524	3721.961	7422.106	12059.772
		TSDT	176.407	1277.057	3727.612	7449.504	12143.407
	0.3	CPT	95.068	760.543	2566.834	6084.347	11883.491
		FSDT	92.766	692.198	2102.364	4375.604	7396.526
		TSDT	92.769	692.342	2104.055	4384.389	7425.807
	0.5	CPT	52.757	422.054	1424.432	3376.432	6594.594
		FSDT	51.767	392.136	1216.305	2590.959	4480.107
		TSDT	51.767	392.184	1216.907	2594.265	4491.730
	0.7	CPT	28.115	224.919	759.103	1799.356	3514.367
		FSDT	27.651	210.793	659.768	1419.893	2480.381
		TSDT	27.651	210.812	659.999	1421.239	2485.328
	0.9	CPT	8.902	71.213	240.345	569.706	1112.708
		FSDT	8.762	66.944	210.195	453.990	795.902
		TSDT	8.762	66.949	210.262	454.382	797.362
T_{cr} (℃)	0.1	CPT	1011.679	4046.716	9105.109	16186.861	25291.970
		FSDT	975.806	3530.766	6863.045	10264.449	13342.182
		TSDT	975.847	3532.214	6873.490	10302.173	13435.085
	0.3	CPT	676.156	2704.621	6085.398	10818.484	16903.881
		FSDT	659.785	2461.568	4984.192	7780.102	10521.189
		TSDT	659.799	2462.088	4988.197	7795.737	10562.787
	0.5	CPT	525.316	2101.264	4727.843	8405.054	13132.896
		FSDT	515.455	1952.305	4037.024	6449.701	8921.895
		TSDT	515.461	1952.549	4039.008	6457.912	8945.031
	0.7	CPT	466.581	1866.324	4199.229	7465.295	11664.523
		FSDT	458.884	1749.114	3649.720	5890.949	8232.639
		TSDT	458.888	1749.265	3651.015	5896.549	8249.044
	0.9	CPT	443.184	1772.735	3988.654	7090.940	11079.594
		FSDT	436.228	1666.464	3488.304	5650.654	7925.057
		TSDT	436.231	1666.590	3489.413	5655.536	7939.595

Also by adding Eqs. (16*c*) and (18*a*), one can obtain:

$$\nabla^2\Psi_1 = \frac{1}{(X+\eta\Phi)}\left\{(\eta^2 F+\eta\Phi)\nabla^4 w^1 - \left[\frac{1}{r}\frac{\partial}{\partial r}\left(rN^0_{rr}\frac{\partial w^1}{\partial r}\right) + \frac{1}{r^2}\frac{\partial}{\partial\theta}\left(N^0_{\theta\theta}\frac{\partial w^1}{\partial\theta}\right) + \frac{2N^0_{r\theta}}{r}\frac{\partial^2 w^1}{\partial r\partial\theta}\right]\right\} \tag{20}$$

Now, by considering Eqs. (16*c*), (18*a*), and (20) and doing some algebraic operations, the following partial differential equation is obtained:

$$(\eta^2 FX-\eta^2\Phi^2)\nabla^6 w^1 - [\Gamma(X+\eta\Phi)-\Gamma(\eta^2 F-\eta\Phi)]\nabla^4 w^1 - (X\nabla^2-\Gamma)\left[\frac{1}{r}\frac{\partial}{\partial r}\left(rN^0_{rr}\frac{\partial w^1}{\partial r}\right) + \frac{1}{r^2}\frac{\partial}{\partial\theta}\left(N^0_{\theta\theta}\frac{\partial w^1}{\partial\theta}\right) + \frac{2N^0_{r\theta}}{r}\frac{\partial^2 w^1}{\partial r\partial\theta}\right] = 0 \tag{21}$$

Eqs. (18*b*) and (21) are two decoupled, partial differential equations in terms of Ψ_2 and w^1. By considering Eqs. (16*a*) and (16*b*), the variations in rotation functions ϕ^1_r and ϕ^1_θ can be written as

$$\phi^1_r = -\frac{\partial w^1}{\partial r} + \frac{X}{\Gamma}\left[\frac{\partial\Psi_1}{\partial r} + \frac{1-\nu}{2}\left(\frac{1}{r}\frac{\partial\Psi_2}{\partial\theta}\right)\right] - \frac{\eta\Phi}{\Gamma}\frac{\partial}{\partial r}(\nabla^2 w^1)$$
$$\phi^1_\theta = -\frac{1}{r}\frac{\partial w^1}{\partial\theta} + \frac{X}{\Gamma}\left[\left(\frac{1}{r}\frac{\partial\Psi_1}{\partial\theta}\right) + \frac{1-\nu}{2}\frac{\partial\Psi_2}{\partial r}\right] - \frac{\eta\Phi}{\Gamma}\frac{1}{r}\frac{\partial}{\partial\theta}(\nabla^2 w^1) \tag{22}$$

For buckling analysis of annular sector plates, the decoupled Eqs. (18*b*) and (20) should be solved.

Buckling Analysis under Mechanical and Thermal Loads

Consider a thick, annular sector plate with arbitrary boundary conditions on inner and outer circular edges subjected to uniform in-plane force P and uniform temperature T. To obtain the critical buckling load and/or temperature, the distribution of the in-plane forces should be determined in the prebuckling configuration. To solve the membrane form of the equilibrium equations, the prebuckling forces are obtained as

Table 10. Comparison among CPT, FSDT, and TSDT for Buckling and Thermal Buckling Analysis of Thick, Annular Sector Plates versus the Variation of h/c and a/b for SSCS ($\beta = 60°$)

Type of loading	a/b	Theory	$h/c = 0.05$	$h/c = 0.1$	$h/c = 0.15$	$h/c = 0.2$	$h/c = 0.25$
N_{cr} (MN)	0.1	CPT	124.916	999.327	3372.728	7994.614	15614.481
		FSDT	121.960	913.684	2791.214	5842.382	9920.525
		TSDT	121.970	913.836	2792.584	5849.688	9945.893
	0.3	CPT	70.763	566.108	1910.613	4528.861	8845.432
		FSDT	69.228	521.861	1615.455	3449.188	5998.348
		TSDT	69.236	522.184	1617.953	3458.737	6023.712
	0.5	CPT	44.534	356.276	1202.432	2850.209	5566.814
		FSDT	43.719	331.847	1033.575	2215.866	3863.657
		TSDT	43.722	331.952	1034.617	2220.842	3879.289
	0.7	CPT	25.934	207.476	700.233	1659.812	3241.821
		FSDT	25.511	194.578	609.580	1313.611	2298.561
		TSDT	25.511	194.605	609.894	1315.339	2304.639
	0.9	CPT	8.701	69.606	234.920	556.848	1087.593
		FSDT	8.564	65.444	205.523	443.997	778.573
		TSDT	8.565	65.450	205.595	444.417	780.123
T_{cr} (°C)	0.1	CPT	691.005	2764.019	6219.043	11056.076	17275.119
		FSDT	674.664	2527.117	5146.702	8079.616	10975.501
		TSDT	674.704	2527.576	5149.344	8089.769	11003.519
	0.3	CPT	503.290	2013.158	4529.606	8052.632	12582.238
		FSDT	492.372	1855.810	3829.854	6132.918	8532.426
		TSDT	492.424	1856.981	3835.808	6149.850	8568.409
	0.5	CPT	443.443	1773.772	3990.985	7095.085	11086.070
		FSDT	435.329	1652.147	3430.547	5516.014	7694.286
		TSDT	435.346	1652.657	3433.991	5528.380	7725.458
	0.7	CPT	430.397	1721.588	3873.572	6886.350	10759.922
		FSDT	423.363	1614.563	3372.091	5450.018	7629.152
		TSDT	423.369	1614.785	3373.837	5457.168	7649.338
	0.9	CPT	433.181	1732.723	3898.627	6930.891	10829.517
		FSDT	426.400	1629.121	3410.767	5526.283	7752.502
		TSDT	426.404	1629.262	3411.968	5531.504	7767.937

$$N^0_{rr} = -P_e \qquad N^0_{\theta\theta} = -P_e \qquad N^0_{r\theta} = 0 \tag{23}$$

where

$$P_e = \begin{cases} P & \text{for mechanical buckling analysis} \\ \frac{T_N}{1-\nu} & \text{for thermal buckling analysis} \end{cases} \tag{24}$$

By substituting Eqs. (23) into Eqs. (18*b*) and (21), the stability equations are obtained as

$$\lambda_1 \nabla^6 w^1 + \lambda_2 \nabla^4 w^1 + \lambda_3 \nabla^2 w^1 = 0 \tag{25}$$

$$\frac{X(1-\nu)}{2} \nabla^2 \Psi_2 - L_{33} \Psi_2 = 0 \tag{26}$$

where the parameters $\lambda_i (i = 1 \ldots 3)$ are defined as

$$\lambda_1 = \frac{\eta^2 (FX - \Phi^2)}{\Gamma}$$
$$\lambda_2 = \frac{XP_e}{\Gamma} - (\eta^2 F + \eta\Phi) - (X + \eta\Phi)$$
$$\lambda_3 = -P_e \tag{27}$$

Levy Solution

It is assumed that the annular sector plate is simply supported in radial edges, and it has arbitrary boundary conditions along the circular edges. For such plate, the transverse displacement w^1 and function Ψ_2 are defined as

Table 11. Variation of Mode Number for Nondimensional Buckling Load for Analysis of Thick, Annular Sector Plate for Various Boundary Conditions ($\beta = 90^\circ$, $h/c = 0.15$, $b/a = 2$)

Boundary condition	Theory	$m = 1$	$m = 2$	$m = 3$	$m = 4$	$m = 5$	$m = 6$	$m = 7$
SSSS	CPT	47.652	68.352	103.022	150.377	208.961	277.673	355.855
	FSDT[a]	44.215	61.552	88.367	121.095	156.418	191.986	226.378
	FSDT[b]	44.173	61.472	88.201	120.784	155.901	191.207	225.295
	TSDT	44.218	61.560	88.391	121.163	156.575	192.300	226.936
SSCC	CPT	152.141	147.752	162.190	197.977	251.899	320.474	401.080
	FSDT[a]	120.115	114.448	123.073	145.270	175.087	207.622	239.988
	FSDT[b]	119.784	114.116	122.698	144.780	174.402	206.678	238.741
	TSDT	120.224	114.666	123.380	145.638	175.564	208.310	241.013
SSFF	CPT	1.860	14.084	35.003	64.069	101.287	146.637	200.084
	FSDT[a]	1.782	13.250	31.539	54.654	81.197	109.838	139.414
	FSDT[b]	1.782	13.243	31.507	54.568	81.019	109.526	138.926
	TSDT	1.878	13.506	31.938	55.207	81.932	110.798	140.661
SSFS	CPT	21.591	53.116	94.293	146.190	207.279	277.084	355.669
	FSDT[a]	19.758	48.718	81.874	118.307	155.414	191.673	226.290
	FSDT[b]	19.742	48.666	81.732	118.010	154.903	190.895	225.207
	TSDT	19.382	48.373	81.745	118.323	155.557	191.983	226.847
SSSF	CPT	3.982	14.979	35.266	64.136	101.302	146.641	200.085
	FSDT[a]	3.872	14.107	31.762	54.700	81.206	109.840	139.414
	FSDT[b]	3.871	14.099	31.730	54.614	81.028	109.527	138.926
	TSDT	3.990	14.371	32.165	55.254	81.940	110.799	140.661
SSFC	CPT	33.675	71.591	117.245	174.257	240.949	316.034	399.474
	FSDT[a]	29.459	61.843	97.317	134.269	171.051	206.343	239.630
	FSDT[b]	29.426	61.744	97.102	133.868	170.407	205.414	238.387
	TSDT	29.029	61.137	96.976	134.305	171.376	206.967	240.628
SSCF	CPT	10.039	17.346	35.968	64.319	101.346	146.651	200.087
	FSDT[a]	9.534	15.984	32.184	54.776	81.217	109.841	139.414
	FSDT[b]	9.529	15.972	32.150	54.689	81.039	109.529	138.926
	TSDT	9.644	16.258	32.593	55.332	81.953	110.801	140.661
SSCS	CPT	78.080	88.996	114.892	156.358	211.609	278.705	356.214
	FSDT[a]	67.674	75.764	95.203	123.847	157.364	192.269	226.453
	FSDT[b]	67.726	75.853	95.316	123.980	157.558	192.600	226.820
	TSDT	67.726	75.853	95.316	123.980	157.557	192.599	226.634
SSSC	CPT	91.670	106.289	137.626	184.881	245.630	317.806	400.072
	FSDT[a]	79.157	89.370	110.757	140.119	173.227	207.040	239.828
	FSDT[b]	79.015	89.184	110.475	139.678	172.564	206.104	238.583
	TSDT	79.185	89.429	110.873	140.338	173.615	207.687	240.844

[a]FSDT $\Rightarrow k^2 = \frac{5}{6}$.
[b]FSDT $\Rightarrow k^2 = \pi^2/12$.

$$w^1 = \sum_{m=1}^{\infty} w_m(r)\sin(\mu_m\theta)$$
$$\Psi_2 = \sum_{m=1}^{\infty} \Psi_m(r)\cos(\mu_m\theta) \tag{28}$$

where μ_m denotes $(m\pi)/\beta$. By substituting Eqs. (28) into Eqs. (25) and (26), two ordinary differential equations are obtained as

$$\lambda_1\frac{d^6w_m(r)}{dr^6}+\frac{3\lambda_1}{r}\frac{d^5w_m(r)}{dr^5}+\gamma_1\frac{d^4w_m(r)}{dr^4}+\gamma_2\frac{d^3w_m(r)}{dr^3}+\gamma_3\frac{d^2w_m(r)}{dr^2}+\gamma_4\frac{dw_m(r)}{dr}+\gamma_5 w_m(r)=0 \tag{29a}$$

$$\frac{X(1-\nu)}{2}\frac{d^2\Psi_m}{dr^2}+\frac{X(1-\nu)}{2r}\frac{d\Psi_m}{dr}+\left(-\Gamma-\frac{X\mu_m^2(1-\nu)}{2r^2}\right)\Psi_m(r)=0 \tag{29b}$$

where the parameters $\gamma_i(i=1,\ldots,5)$ are defined as

$$\begin{aligned}
\gamma_1 &= \lambda_2-\frac{3\lambda_1\mu_m^2}{r^2}-\frac{3\lambda_1}{r^2}\\
\gamma_2 &= \frac{6\lambda_1}{r^3}+\frac{6\lambda_1\mu_m^2}{r^3}+\frac{2\lambda_2}{r}\\
\gamma_3 &= \lambda_3-\frac{21\lambda_1\mu_m^2}{r^4}-\frac{9\lambda_1}{r^4}-\frac{2\lambda_2\mu_m^2}{r^2}+\frac{3\lambda_1\mu_m^4}{r^4}-\frac{\lambda_2}{r^2}\\
\gamma_4 &= \frac{45\lambda_1\mu_m^2}{r^5}+\frac{\lambda_2}{r^3}+\frac{\lambda_3}{r}+\frac{9\lambda_1}{r^5}-\frac{9\lambda_1\mu_m^4}{r^5}+\frac{2\lambda_2\mu_m^2}{r^3}\\
\gamma_5 &= \frac{\lambda_2\mu_m^4}{r^4}-\frac{\lambda_1\mu_m^6}{r^6}-\frac{4\lambda_2\mu_m^2}{r^4}+\frac{20\lambda_1\mu_m^4}{r^6}-\frac{64\lambda_1\mu_m^2}{r^6}-\frac{\lambda_3\mu_m^2}{r^2}
\end{aligned} \tag{30}$$

The solutions of ordinary differential Eqs. (29) are as follows [see Watson (1922) and Wang et al. (2000)]:

$$\begin{aligned}
w_m(r) = {} & C_1r^{\mu_m}+C_2r^{-\mu_m}+C_3I_{\mu_m}\left(\sqrt{\frac{-\lambda_2-\sqrt{4\lambda_3\lambda_1+\lambda_2^2}}{2\lambda_1}}r\right)\\
& +C_4J_{\mu_m}\left(\sqrt{\frac{\lambda_2-\sqrt{-4\lambda_3\lambda_1+\lambda_2^2}}{2\lambda_1}}r\right)\\
& +C_5K_{\mu_m}\left(\sqrt{\frac{-\lambda_2-\sqrt{-4\lambda_3\lambda_1+\lambda_2^2}}{2\lambda_1}}r\right)\\
& +C_6Y_{\mu_m}\left(\sqrt{\frac{\lambda_2-\sqrt{4\lambda_3\lambda_1+\lambda_2^2}}{2\lambda_1}}r\right)
\end{aligned} \tag{31}$$

$$\Psi_m(r)=C_7I_{\mu_m}\left(\sqrt{\frac{2\Gamma}{X(1-\nu)}}r\right)+C_8K_{\mu_m}\left(\sqrt{\frac{2\Gamma}{X(1-\nu)}}r\right) \tag{32}$$

where J and Y are the Bessel functions and I and K are the modified Bessel functions. $C_i(i=1\ldots8)$ are eight unknown constants, and the parameters λ_1, λ_2, and λ_3 have been defined in Eqs. (27). By satisfying the boundary conditions in circular edges, eight algebraic equations in terms of unknown coefficients C_i are obtained. To set the determinant of coefficients of these equations equal to zero, the critical buckling load and/or temperature for annular sector plate is determined.

Boundary Conditions

For circular edges of annular sector plates, the boundary conditions can be simply supported, clamped, and free. Simply supported boundary condition in circular edges requires

$$w_m^1 = M_{rr}^1 = P_{rr}^1 = \phi_\theta^1 = 0 \tag{33}$$

Also, for clamped boundary condition in circular edges, it can be written

$$w_m^1 = \phi_r^1 = \phi_1^\theta = \frac{dw^1}{dr} = 0 \tag{34}$$

If the circular edges are free, it is reasonable to have

$$M_{rr}^1 = P_{rr}^1 = \hat{M}_{r\theta}^1 = \hat{Q}_r^1+\eta\left(\frac{dP_{rr}}{dr}+\frac{2}{r}\frac{dP_{r\theta}}{d\theta}+\frac{P_{rr}-P_{\theta\theta}}{r}\right)+P_e\frac{dw^1}{dr}=0 \tag{35}$$

where $\hat{Q}_r$ is defined as follows:

$$\hat{Q}_r^1 = \Gamma\left(\frac{\partial w^1}{\partial r}+\phi_r^1\right) \tag{36}$$

It is assumed that the radial edges of annular sector plate are simply supported and the boundary conditions along the circular edges are identified according to the inner and outer radius of the plate. The nine possible boundary conditions containing SSSS, SSCC, SSFF, SSCF, SSFC, SSCS, SSSC, SSSF, and SSFS have been considered for obtaining the numerical results (e.g., SSCF denotes an annular sector plate with simply supported radial edges, clamped inner and free outer circular edges).

Numerical Results and Discussion

In this section, the numerical results have been presented for thick, annular sector plates with nine possible boundary conditions along the circular edges. The material properties of the plate are as follows: $E=380$ GPa, $\nu=0.3$, and $\alpha=7.6\times10^6(1/°C)$.

Table 1 shows the comparison of the buckling loads with those reported by Wang and Xiang (1999) for complete sector plates based on FSDT. For this comparison, the inner radius is considered very small (e.g., $a=1\times10^{-10}$). Based on Table 1, the present results are in good agreement. So, the presented formulations are reliable.

Tables 2–10 present the critical buckling load and temperature of annular sector plates under various boundary conditions versus the thickness/length ratio, h/c, $(c=b-a)$ and aspect ratio, a/b, based on the CPT, FSDT, and TSDT. In these tables, the numbers in the parentheses show the mode number. If any number was not presented, the first mode has been considered (i.e., $m=1$).

Table 2 presents the critical buckling load and temperature for simply supported annular sector plates. Note that the critical buckling load and temperature increase with the increase of thickness/length ratio. Also, the increase of aspect ratio, a/b, leads to decrease, in the critical buckling load and temperature in all three theories. By comparison of the results obtained for all theories, it could be observed that an increase in the thickness causes to increase the difference between the results of CPT and two others. Also, for the SSSS boundary condition, the results

of FSDT and TSDT are almost close to each other, even for thick plates.

Table 3 presents the critical buckling load and temperature of annular sector plate for the SSCC boundary condition. The critical buckling load and temperature increase with the increase in thickness/length ratio. Also, the increase of aspect ratio, a/b, leads to a decrease in the critical buckling load. This behavior is not seen for the critical buckling temperature because, by increasing the aspect ratio, the critical buckling temperature decreases only for $a/b < 0.7$. By increasing the aspect ratio, the mode number changes. For instance, in $a/b = 0.9$, both the critical buckling load and temperature occur in the 7th mode number. From Tables 2 and 3, it can be seen that in the minimum value for buckling load and temperature is predicted by FSDT, and the maximum value is predicted by CPT. Also, for thick plates, the results of FSDT are close to those of TSDT.

Tables 4–6 present the critical buckling load and temperature of annular sector plate for SSFF, SSSF, and SSCF boundary conditions, respectively. It can be deduced from these tables that the critical buckling load and temperature decrease with the increase of aspect ratio, and they increase with an increase in the thickness/length ratio. Also, in boundary conditions containing free edges in outer radius, the predicted values of TSDT are larger than those of other theories for $h/c \leq 0.05$. Another noticeable point is that the results of CPT for plates containing free boundary conditions are acceptable in the range $h/c \leq 0.15$.

Tables 7 and 8 present the critical buckling load and temperature of annular sector plates for SSFS and SSFC boundary conditions. It can be seen that increasing the aspect ratio leads to a decrease in the critical buckling load and temperature, and increasing the thickness/length ratio causes the critical buckling load and temperature to increase. For these boundary conditions with $h/c = 0.05$, the minimum value for critical buckling load and temperature is predicted by TSDT and the maximum value is predicted by CPT.

Tables 9 and 10 present the critical buckling load and temperature of annular sector plates for SSSC and SSCS boundary conditions. It can be seen that by increasing the aspect ratio and/or thickness/length ratio, the critical buckling load and temperature increases. Certainly, for boundary conditions containing clamped edges, the results of CPT are acceptable when $h/c \leq 0.1$.

It can be found from Tables 2–10 that the difference between first- and third-order shear deformation theories is more significant for annular sector plates containing clamped boundary condition, and the difference increases by increasing the thickness/radius ratio.

Table 11 presents the nondimensional buckling load for nine different boundary conditions versus the variation of mode

Table 12. Critical Buckling Temperature of Annular Sector Plate for Various Boundary Conditions versus β and a/b ($h/c = 0.1$)

β	a/b	Theory	SSSS	SSCC	SSFF	SSFS	SSSF	SSCF	SSFC	SSSC	SSCS
60°	0.3	CPT	1765.439	3242.097	146.647	1614.642	322.636	345.712	2366.098	2704.621	2013.158
		FSDT	1667.202	2843.340	142.465	1530.031	311.893	330.519	2177.664	2461.568	2013.158
		TSDT	1667.269	2846.175	146.331	1527.054	320.336	339.089	2170.184	2462.088	1856.981
	0.7	CPT	958.909	3215.201(2)	45.252	210.647	78.269	236.380	401.993	1866.324	1721.588
		FSDT	929.392	2859.536(2)	44.156	200.904	76.484	230.379	381.966	1749.114	1614.563
		TSDT	929.403	2860.534(2)	45.434	198.314	77.841	231.596	379.495	1749.265	1614.785
90°	0.3	CPT	1294.893	3166.312	95.926	1027.488	131.541	199.397	1734.923	2287.938	1716.021
		FSDT	1240.083	2799.026	93.199	993.610	128.949	190.642	1625.381	2113.449	1591.290
		TSDT	1240.112	2800.894	98.099	985.764	134.529	196.222	1605.278	2113.712	1592.202
	0.7	CPT	905.749	3215.201(3)	11.693	106.443	40.120	219.882	313.243	1842.680	1702.990
		FSDT	999.338	2851.421(4)	11.397	101.704	39.375	216.304	302.727	1729.585	1599.445
		TSDT	879.364	2852.962(4)	12.045	100.333	40.076	216.893	301.498	1729.714	1599.631
120°	0.3	CPT	1137.868	2949.273	27.373	800.208	85.019	185.494	1466.699	2180.695	1647.442
		FSDT	1094.651	2843.340(2)	26.506	774.864	83.744	178.852	1354.181	2024.619	1533.252
		TSDT	1094.676	2846.175(2)	29.191	763.308	87.760	182.665	1325.880	2024.805	1533.938
	0.7	CPT	887.177	3213.295(5)	2.971	66.080	26.902	215.267	280.816	1835.168	1697.192
		FSDT	861.833	2844.412(5)	2.893	63.317	26.490	212.596	273.957	1723.461	1594.832
		TSDT	861.854	2845.813(5)	3.212	62.490	26.909	212.938	273.236	1723.583	1595.005
270°	0.3	CPT	989.958	3166.312(3)	12.744(2)	387.863	77.954(2)	188.870(2)	773.533	2118.308	1610.545
		FSDT	956.387	2795.263(4)	12.313(2)	359.516	76.901(2)	182.991(2)	706.611	1976.996	1507.447
		TSDT	956.401	2797.857(4)	12.230	349.231	80.363(2)	186.182(2)	693.886	1977.117	1507.828
	0.7	CPT	868.035	3207.219(10)	1.328(2)	21.541	13.361	211.230	246.468	1827.870	1691.626
		FSDT	843.751	2843.498(11)	1.292(2)	20.970	13.279	209.534	243.598	1717.563	1590.468
		TSDT	843.760	2844.851(11)	1.085	20.794	13.367	209.604	243.449	1717.676	1590.629
360°	0.3	CPT	975.477	3163.297(5)	34.917	285.265	76.370(2)	185.494(3)	635.167	2116.034	1609.245
		FSDT	942.794	2784.030(5)	33.393	264.678	75.596(2)	178.852(3)	591.797	1975.991	1507.357
		TSDT	942.810	2786.469(5)	30.233	257.833	77.907(2)	201.558(2)	584.094	1976.107	1507.703
	0.7	CPT	865.975	3207.377(14)	3.029	16.540	11.909	210.842	242.710	1827.112	1691.052
		FSDT	841.804	2843.725(14)	2.950	16.216	11.862	209.253	240.284	1716.954	1590.023
		TSDT	841.805	2844.985(14)	2.631	16.116	11.912	209.293	240.199	1717.067	1590.183

number. For comparison, two values for the shear correction factor, $k^2 = 5/6$ and $\pi^2/12$, have been used in FSDT. As it can be observed from the table, for the majority of boundary conditions and the shear correction factor $k^2 = 5/6$, FSDT gives the results that are close to those obtained by TSDT. Also, it is clear that in large mode numbers, the effect of inner boundary condition is negligible.

Table 12 presents the critical buckling temperature of annular sector plates versus the variation of sector angle and aspect ratio. It can be seen that except for SSFF and SSCF boundary conditions, by increasing the sector angle, the critical buckling temperature decreases. Also, by increasing the sector angle, the mode number in which the bucking occurred increases. For example, for a plate with SSCC boundary condition, $\beta = 360^{\circ}$ and $a/b = 0.7$, the minimum mode number is $m = 14$. A significant point in this table is that the mode numbers predicted by different theories are not the same. For example, for plates with SSCC boundary condition ($\beta = 90^{\circ}$, $a/b = 0.7$; $\beta = 120^{\circ}$, $a/b = 0.3$; and $\beta = 270^{\circ}$, $a/b = 0.3, 0.7$), the mode numbers predicted by CPT are different than those predicted by FSDT and TSDT.

Fig. 2 shows the critical buckling temperature of an annular sector plates versus the sector angle β and aspect ratio a/b for SSSS boundary condition. It can be seen from this figure that increasing the sector angle leads to a decrease in the critical buckling temperature. Also by increasing the aspect ratio, the critical buckling temperature increases. A significant note in this figure is that the

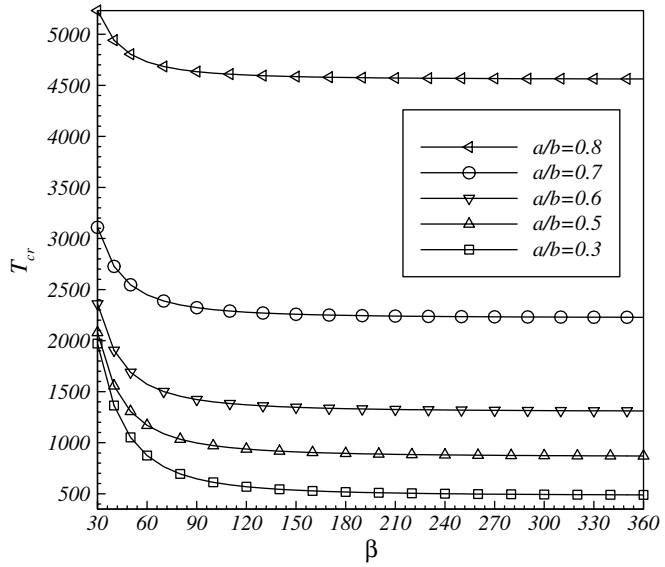

Fig. 2. Critical buckling temperature of annular sector plate versus sector angle β and a/b for SSSS boundary condition ($b/h = 20$)

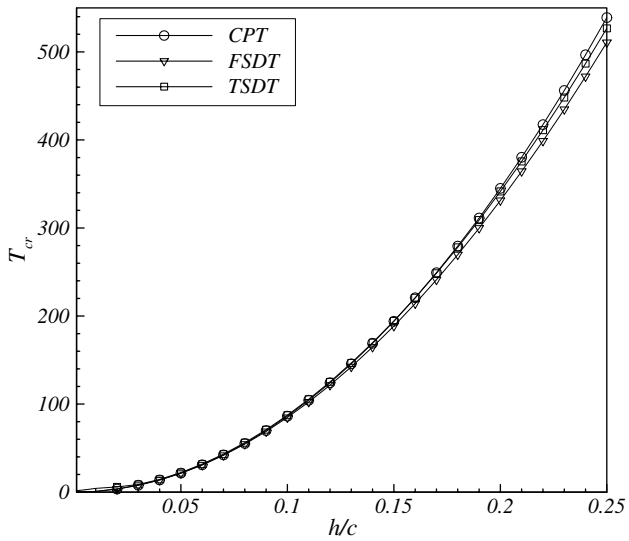

Fig. 4. Critical buckling temperature of annular sector plate versus sector angle h/c for SSSF boundary condition ($a/b = 0.5$, $\beta = 90°$)

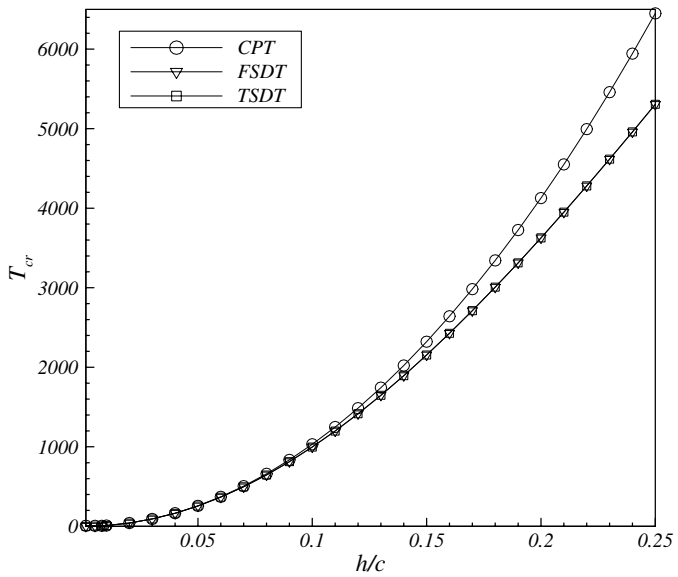

Fig. 3. Critical buckling temperature of annular sector plate versus sector angle h/c for SSSS boundary condition ($a/b = 0.5$, $\beta = 90°$)

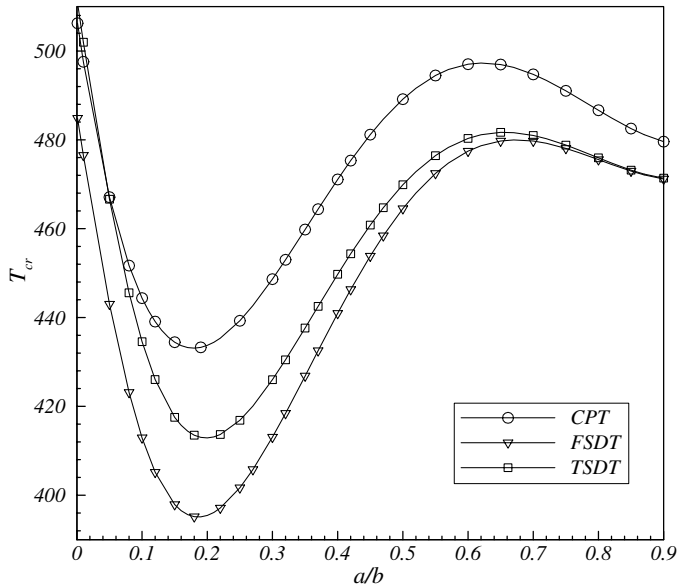

Fig. 5. Critical buckling temperature of annular sector plate versus sector angle a/b for SSCF boundary condition ($h/c = 0.15$, $\beta = 90°$)

difference among the values of critical buckling temperature increases drastically for $a/b > 0.7$.

Fig. 3 shows the critical buckling temperature of an SSSS annular sector plate based on different theories versus the thickness/length ratio. It can be seen that for this boundary condition, by increasing the thickness/length ratio, the results of CPT deviate from those of the other theories.

Fig. 4 shows the critical buckling temperature of a SSSF annular sector plate based on different theories. It can be seen that for this boundary condition, the results of all presented theories are almost close to each other. In other words, the results of CPT are reliable for SSSF annular sector plates.

Fig. 5 shows the critical buckling temperature of a SSCF annular sector plate based on different theories versus the aspect ratio. It can be seen that the results of TSDT for $a/b < 0.15$ are closer to those obtained by CPT; however, for $a/b > 0.5$, they are closer to those obtained by FSDT.

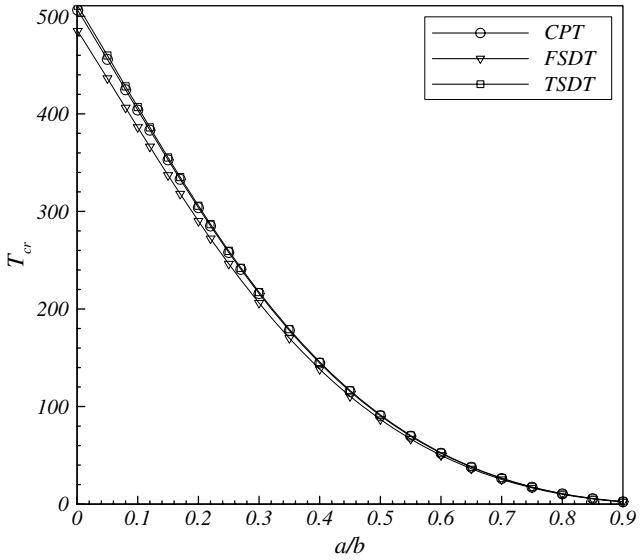

Fig. 6. Critical buckling temperature of annular sector plate versus sector angle a/b for SSFF boundary condition ($h/c = 0.15$, $\beta = 90°$)

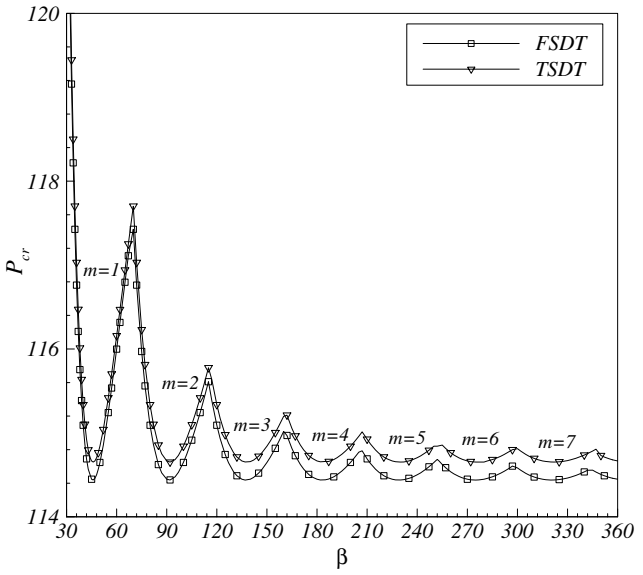

Fig. 7. Critical buckling temperature of annular sector plate versus sector angle β for SSCC boundary condition ($a/b = 0.5$, $h/c = 0.15$)

Fig. 6 shows the critical buckling temperature of a SSFF annular sector plate for all three theories versus the aspect ratio. It can be seen that for this boundary condition, the results obtained by TSDT are close to those obtained by CPT in smaller values of aspect ratio. Also, for larger values of aspect ratio, all three theories give close results for critical buckling temperature.

Fig. 7 shows the nondimensional critical buckling load of an annular sector plate versus the sector angle for SSCC boundary condition. It can be seen that the results obtained by FSDT and TSDT are close to each other when $m = 1$ and their difference increases by increasing the mode number.

Conclusions

In this paper, the stability equations of thick, annular sector plates based on TSDT have been decoupled and solved analytically for the first time. The numerical results for critical buckling load/temperature of annular sector plates with nine different boundary conditions has been presented. Comparisons for the critical buckling load and/or temperature of the annular sector plates have been investigated with those obtained based on CPT and FSDT. The effects of boundary conditions, thickness/radius ratio, sector angle, and annularity on the buckling load/temperature of annular sector plate have been discussed. and the range of validity of plate theories for buckling analysis of thick, annular sector plates under different boundary conditions has been specified. The following conclusions can be remarked:

1. For boundary conditions containing simply supported and clamped edges, the minimum value for buckling load/temperature is predicted by FSDT and the maximum value is predicted by CPT.
2. For boundary conditions containing free edges, the critical buckling load/temperature predicted by TSDT is larger than those obtained using other theories for $h/c = 0.05$.
3. For annular sector plates containing free edges, the results predicated by CPT are acceptable if $h/c \leq 0.15$.
4. For annular sector plates containing clamped edges, the results predicated by CPT are acceptable if $h/c \leq 0.1$.
5. For the majority of boundary conditions, in the buckling analysis of annular sector plates, the shear correction factor $k^2 = 5/6$ is more appropriate than $k^2 = \pi^2/12$.
6. In large mode numbers, the effect of inner boundary condition is negligible.
7. For SSCC boundary condition, by increasing the aspect ratio, the critical buckling load decreases but the critical buckling temperature decreases and then increases.
8. By increasing the sector angle, the critical mode number increases.
9. For some cases, the critical mode numbers predicted by different theories are not the same.

References

Bodaghi, M., and Saidi, A. R. (2010). "Levy-type solution for buckling analysis of thick functionally graded rectangular plates based on the higher-order shear deformation plate theory." *Appl. Math. Modell.*, 34(11), 3659–3673.

Brush, D. O., and Almroth, B. O. (1975). Chapter 3, *Buckling of bars, plates and shells*, McGraw-Hill, New York.

Javaheri, R., and Eslami, M. R. (2002). "Thermal of functionally graded plates based on higher order theory." *J. Therm. Stress.*, 25(7), 603–625.

Levinson, M. (1980). "An accurate simple theory of the statics and dynamics of elastic plates." *Mech. Res. Commun.*, 7(6), 343–350.
Liu, W. H., and Chen, W. C. (1989). "Note on the stability of annular sector plates with elastically restrained edges." *Int. J. Mech. Sci.*, 31(8), 611–622.
Mindlin, R. D. (1951). "Influence of rotary inertia and shear on flexural motions of isotropic, elastic plates." *J. Appl. Mech.*, 18, 1, 31–38.
Naderi, A., and Saidi, A. R. (2011a). "An analytical solution for buckling of moderately thick functionally graded sector and annular sector plates." *Arch. Appl. Mech.*, 81(6), 809–828.
Naderi, A., and Saidi, A R. (2011b). "Exact solution for stability analysis of moderately thick functionally graded sector plates on elastic foundation." *Compos. Struct.*, 93(2), 629–638.
Navaneethakrishnan, P. V. (1988). "Buckling of nonuniform plates: Spline method." *Eng. Mech.*, 114(5), 893–898.
Ni, Q. Q., Xie, J., and Iwamoto, M. (2005). "Buckling analysis of laminated composite plates with arbitrary edge supports." *Compos. Struct.*, 69(2), 209–217.
Nosier, A., and Reddy, J. N. (1992a). "On vibration and buckling of symmetric laminated plates to shear deformation theories according to shear deformation theories. Part I." *Acta Mech.*, 94(3–4), 123–144.
Nosier, A., and Reddy, J. N. (1992b). "On vibration and buckling of symmetric laminated plates to shear deformation theories according to shear deformation theories. Part II." *Acta Mech.*, 94(3–4), 145–169.
Reddy, J. N. (1984a). "A simple higher-order theory for laminated plates." *J. Appl. Mech.*, 51(4), 745–752.
Reddy, J. N. (1984b) "A refined nonlinear theory of plates with transverse shear deformation." *Int. J. Solids Struct.*, 20(9–10), 881–896.
Reddy, J. N., and Liu, C. F. (1985). "A higher-order shear deformation theory of laminated elastic shells." *Int. J. Eng. Sci.*, 23(3), 319–330.
Reddy, J. N., and Phan, N. D. (1985). "Stability and vibration of isotropic, orthotropic and laminated plates according to a higher-order shear deformation theory." *J. Sound Vib.*, 98(2), 157–170.
Reissner, E. (1945). "The effect of transverse shear deformation on the bending of elastic plates." *J. Appl. Mech.*, 12(2), 69–77.
Rubin, C. (1978). "Stability of polar orthotropic sector plates." *J. Appl. Mech.*, 45(2), 448–450.
Saidi, A. R., and Hasani Baferani, A. (2010). "Thermal buckling analysis of moderately thick functionally graded annular sector plates." *Compos. Struct.*, 92(7), 1744–1752.
Saidi, A. R., Rasouli, A., and Sahraee, S. (2009). "Axisymmetric bending and buckling analysis of thick functionally graded circular plates using unconstrained third-order shear deformation plate theory." *Compos. Struct.*, 89(1), 110–119.
Samsam Shariat, B. A., and Eslami, M. R. (2007). "Buckling of thick functionally graded plates under mechanical and thermal loads." *Compos. Struct.*, 78(3), 433–439.
Sharma, A., Sharda, H. B., and Nath, Y. (2005a). "Stability and vibration of Mindlin sector plates: An analytical approach." *AIAA J.*, 43(5), 1109–1116.
Sharma, A., Sharda, H. B., and Nath, Y. (2005b). "Stability and vibration of thick laminated composite sector plates." *J. Sound Vib.*, 287(1–2), 1–23.
Srinivasan, R. S., and Thiruvenkatachari, V. (1984). "Stability of annular sector plates with variable thickness." *AIAA J.*, 22(2), 315–317.
Wang, C. M., and Lee, K. H. (1998). "Buckling load relationship between Reddy and Kirchhoff circular plates." *J. Franklin Inst.*, 335(6), 989–995.
Wang, C. M., Reddy, J. N., and Lee, K. H. (2000). *Shear deformable beams and plates: Relationships with classical solutions*, Elsevier, Oxford, UK.
Wang, C. M., and Xiang, Y. (1999). "Deducing buckling loads of sectorial Mindlin plates from Kirchhoff plates." *Eng. Mech.*, 125(5), 596–598.
Wang, C. M., Xiang, Y., Kitipornchai, S., and Liew, K. M. (1994). "Buckling solutions for Mindlin plates of various shapes." *Eng. Struct.*, 16(2), 119–127.
Watson, N. G., (1922). *Theory of Bessel functions*, Cambridge University Press, Cambridge.
Zhou, Y. H., Zheng, X., and Hariky, I. E. (1995). "A seminumerical method for buckling of sector plates." *Comput. Struct.*, 57(5), 847–854.